AD-A128 727 LASER-CONTROLLED MILLIMETER-WAVE SWITCHING GATING AND PHASE SHIFTING IN DIELECTRIC WAVEGUIDES(U) MARYLAND UNIV COLLEGE PARK DEPT OF ELECTRICAL ENGINEERING C H LEE MAY 83 1/1

UNCLASSIFIED F/G 9/5 NL

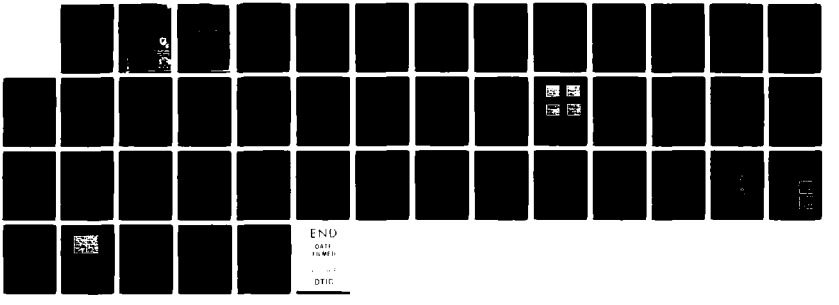

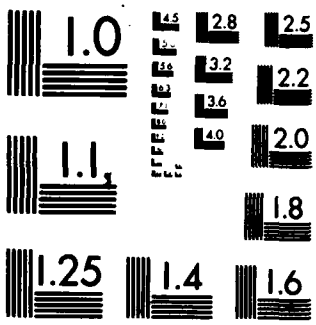

MICROCOPY RESOLUTION TEST CHART
NATIONAL BUREAU OF STANDARDS-1963-A

HDL-CR-83-109-1

May 1983

Laser-Controlled Millimeter-Wave Switching, Gating, and Phase Shifting in Dielectric Waveguides

by Chi H. Lee

AD A128727

Prepared by

Department of Electrical Engineering
University of Maryland
College Park, MD 20742

Under contract

DAAK21-81-C-0109

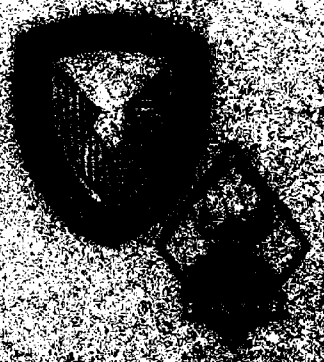

U.S. Army Electronics Research
and Development Command
Harry Diamond Laboratories

Approved for public release; distribution unlimited.

DTIC COPY

The findings in this report are not to be construed as an official Department of the Army position unless so designated by other authorized documents.

Citation of manufacturers' or trade names does not constitute an official indorsement or approval of the use thereof.

Destroy this report when it is no longer needed. Do not return it to the originator.

Unclassified

SECURITY CLASSIFICATION OF THIS PAGE (When Data Entered)

REPORT DOCUMENTATION PAGE	READ INSTRUCTIONS BEFORE COMPLETING FORM
1. REPORT NUMBER: HDL-CR-83-109-1 — 2. GOVT ACCESSION NO.: AD-A128727	3. RECIPIENT'S CATALOG NUMBER
4. TITLE (and Subtitle): Laser-Controlled Millimeter-Wave Switching, Gating, and Phase Shifting in Dielectric Waveguides	5. TYPE OF REPORT & PERIOD COVERED: Contractor Report 6. PERFORMING ORG. REPORT NUMBER
7. AUTHOR(s): Chi H. Lee (HDL contact: Mary Tobin)	8. CONTRACT OR GRANT NUMBER(s): DAAK21-81-C-0109
9. PERFORMING ORGANIZATION NAME AND ADDRESS: Department of Electrical Engineering University of Maryland College Park, MD 20742	10. PROGRAM ELEMENT, PROJECT, TASK AREA & WORK UNIT NUMBERS: Program el: 61102A
11. CONTROLLING OFFICE NAME AND ADDRESS: Commander Harry Diamond Laboratories Adelphi, MD 20783	12. REPORT DATE 13. NUMBER OF PAGES
14. MONITORING AGENCY NAME & ADDRESS (if different from Controlling Office)	15. SECURITY CLASS. (of this report): UNCLASSIFIED 15a. DECLASSIFICATION/DOWNGRADING SCHEDULE

16. DISTRIBUTION STATEMENT (of this Report)

Approved for public release; distribution unlimited.

17. DISTRIBUTION STATEMENT (of the abstract entered in Block 20, if different from Report)

18. SUPPLEMENTARY NOTES

HDL project: 314132
DRCMS code: 6111020000000

19. KEY WORDS (Continue on reverse side if necessary and identify by block number)

Waveguides, millimeter wave propagation

20. ABSTRACT (Continue on reverse side if necessary and identify by block number)

The results are summarized of the investigation of a number of millimeter-wave device concepts based on laser-induced solid-state plasma in a semiconducting waveguide. Using the waveguide as a phase shifter, a phase shift up to 1400°/cm has been obtained. Using a Cr-doped GaAs waveguide, a millimeter-wave modulator with a bandwidth greater than 1 GHz has been demonstrated. A

DD FORM 1 JAN 73 1473 EDITION OF 1 NOV 65 IS OBSOLETE

Unclassified

1

SECURITY CLASSIFICATION OF THIS PAGE (When Data Entered)

20. complete theoretical analysis has been carried out and a dynamic bridge method has been devised to measure the rapid phase change. Several experiments are suggested for future study. The ultimate goal of this research is to develop a monolithic millimeter-wave integrated circuit technology. The results of this study show that this goal is clearly achievable.

Accession For
NTIS GRA&I [X]
DTIC TAB [ ]
Unannounced [ ]
Justification
By
Distribution/
Availability Codes
Dist | Avail and/or Special
A

CONTENTS

APPENDICES

83 05 27

FIGURES

1. Introduction

Contract DAAK21-81-C-0109 was awarded on September 17, 1981, for the study of the switching, gating, and phase shifting of millimeter waves in semiconductor waveguides by a laser-induced electron hole plasma. Before this contract, preliminary work had been performed and the results were reported elsewhere. We reported[1] the demonstration of a new method for controlling millimeter-wave propagation in a semiconductor waveguide, i.e., optical control. A phase shift of 300^{o}/cm at 94 GHz was observed. A simple theory was developed to explain the observed behavior. This technique was also extended to ultra-fast switching and gating of millimeter-wave signals. Millimeter-wave pulsewidths as short as 1ns and variable to several tens of nanoseconds were observed.

The main objective of the current contract is to further advance the state of the art in this area by performing the following specific tasks:

(1) setting up a 94 GHz system for parameter measurements,

(2) fabricating different waveguides from Si and GaAs,

(3) measuring the phase shift and attenuation as a function of the laser-induced plasma in various waveguides, with particular emphasis on waveguides operated close to cutoff,

(4) measuring these parameters as a function of laser wavelength and pulsewidth, and

(5) developing a theoretical model and computer code to facilitate comparison between theory and experiment.

The contract allowed for some deviation from these specific tasks if a particular avenue of research was found to be especially fruitful. It was intended that this research should be published in respected technical journals.

Our research has been quite successful. We have accomplished all the tasks listed above except for measuring the phase shift and attenuation as a function of laser pulsewidth (This information is not critical for the understanding of the physics of the devices). In addition, a dynamic bridge method has been developed which, for the first time, can monitor the rapid change of phase and attenuation at a subnanosecond time scale at 94 GHz. Chirped millimeter-wave pulses have been observed in a GaAs waveguide with potential for further compression of the pulses for millimeter-wave radar applications. We have also demonstrated the wideband modulation of millimeter waves with a bandwidth in excess of 1 GHz. A phase shift as high as 1400^{o}/cm has been observed.

A parallel effort in the theoretical description of these devices has been carried out. A computer code has been developed to analyze higher order modes of propagation in the plasma-controlled region of both Si and GaAs waveguides at various frequencies and for various waveguide dimensions. We have also for-

[1] Chi H. Lee, P. S. Mak, and A. P. DeFonzo, "Optical control of millimeter wave propagation in dielectric waveguides," IEEE J. Quantum Electron QE-16 (1980), 277-288.

mulated a surface plasma model that is a good approximation of the more elaborate volume plasma model. This model will facilitate, in future research, the computation of a more complicated situation where mode coupling effects may be important.

Our research has resulted in several publications. They are as follows:

(1) Theory of optically controlled millimeter-wave phase shifters, published in the IEEE Transactions on Microwave Theory and Techniques in a special issue on millimeter waves, MTT-31, 209-216, (February, 1983).

(2) Wide bandwidth high repetition-rate optoelectronic modulation of millimeter-waves in GaAs waveguide, Electronics Letters, 18 454; (May 1982), and

(3) Picosecond optoelectronic modulation of millimeter-waves in GaAs waveguide, accepted for publication in Picosecond Phenomena III, edited by R. M. Hochstrasser and W. Kaiser, Springer-Verlag, 1982, 145-148.

The reprints of these papers are included as appendices. Anyone who is interested in the technical details should consult these appendices.

In section 2, the background and a historical overview of this research field is presented. Technical descriptions and results are in section 3. Section 3.1 discusses the concept of optical control of millimeter-wave propagation and Section 3.2 gives a summary of the theoretical analysis. The dynamic bridge method for measuring the rapid change of phase and attenuation as a function of time is presented in detail in Section 3.3. Highlights of the current research results are listed in Section 3.4. Section 4 contains suggestions for future research topics.

With better understanding of the physics of these devices, we believe that it is now possible to build a monolithic millimeter-wave integrated circuit technology based on this foundation. The approach of using a solid-state plasma as a means of control (this also includes the PIN diode work done by Jacobs et al[2]) appears to be the only successful one so far. Continued funding of this effort is needed to advance this research to a stage where this technology can be transferred to industry for system development.

2. Background

We are currently witnessing a resurgence of interest in millimeter-wave technology. The frequency band extending from 30 to 1000 GHz is attractive in several respects. Devices operating above K band frequencies offer the benefits of greater carrier bandwidth, better spatial resolution, and a more compact technology than presently used X and K band systems. On the other hand, millimeter and submillimeter wave systems have some advantages over optical systems: better atmospheric propagation through fogs and smokes in selected

[2] H. Jacobs and M. M. Chrepta, "Electronic phase shifter for millimeter-wave semiconductor dielectric integrated circuits," IEEE Trans. Microwave Theory Tech, MTT-22 (1974), 411-417.

bands and a technology more amenable to frequency multiplexing[3-5] but retaining the good angular resolution of the latter. An outstanding and basic problem is how to effectively preserve these benefits. Our approach to the solution of this problem promises to yield much larger modulation bandwidths than are realizable with optical techniques while preserving economy over a given carrier frequency band.

One of the important parts of microwave and millimeter wave systems is the waveguide. At microwave frequencies, metal waveguides are commonly used. At higher frequencies, either microstrip or dielectric waveguide structures become more attractive. Both of these structures can be fabricated by integrated circuit techniques. Complex millimeter-wave integrated circuit elements can be easily formed from dielectric materials by employing batch fabrication techniques using sandblasting, machining, laser cutting, etc. Microstrip transmission lines are used up to 30 GHz. For frequencies greater than 30 GHz, the losses in microstrip structures are high and fabrication techniques become more difficult because of the narrow strips and the substrate thickness. Dielectric rectangular waveguides become, then, the only alternative to the expensive metal waveguides. The use of high-purity semiconductor materials as dielectric waveguides is particularly important since active devices, such as oscillators, Gunn or IMPATT diodes, mixers/detectors, and modulators, can all be fabricated in situ into the semiconducting waveguides.

One important aspect of millimeter-wave devices is the control of phase and amplitude of a wave propagating through the waveguide. Such devices with a reasonable speed and acceptable bandwidth are not yet available in the millimeter-wave region. The use of semiconductor bulk phenomena in implementing microwave control components has been discussed[6]. The principal phenomena explored have been the dielectric and conductive properties of the plasma states. A frequency-scanning millimeter-wave antenna utilizing periodic metallic stripe perturbations on a silicon waveguide has been demonstrated[7]. Millimeter-wave dielectric image-guide integrated devices have been developed[8]. At the optical region, there are various controllable wave guide devices which have not found their counterparts in the millimeter-wave region. High-speed light modulators that make use of the electro-optic, acousto-optic, and magneto-optic effects in bulk material have been described[9]. All these effects

---

[3] W. J. Tomlinson, "Wavelength multiplexing in multimode optical fibres,", Appl. Opt. 16 (1977), 2180-2194.

[4] M. Kobayashi and H. Herui, "Optical demultiplexer using coupling between nonidentical waveguides," Appl. Opt. 17 (1978), 3253-3258.

[5] J. Minowa, K. Aoyama, and Y. Fujii, "Silicon blazed-grating for low loss optical multiplexer," 1979 IEEE/OSA Conference on Laser Engineering and Applications, Digest of Technical Papers, paper 3.10 (1979), 54-55.

[6] K. E. Mortenson, A. L. Armstrong, J. M. Borrego, and J. F. White, "A review of bulk semiconductor microwave control components," Proc IEEE, 59 (1971), 1191-1200.

[7] K. L. Klohn, R. E. Horn, H. Jacobs, and E. Friebergs, "Silicon waveguide frequency scanning linear array antenna," IEEE Trans. Microwave Theory Tech., MTT-26 (1978), 764-773.

[8] J. A. Paul and Y. W. Chang, "Millimeter-wave image-guide integrated passive devices," IEEE Trans. Microwave Theory Tech., MTT-26 (1978), 751-754.

[9] I. P. Kaminow, "Optical waveguide modulators," IEEE Trans. Microwave Theory Tech., MTT-23 (1975), 57-70.

produce refractive index changes and, in turn, modify the characteristics of the propagating fields. Within these general principles, an electro-optic multimode waveguide switch based on nonuniform modulations of the refractive-index profile of the active waveguide at optical wavelengths has recently been demonstrated[10]. A Mach-Zehnder interferometric integrated-optical waveguide modulator has also been reported[11].

Phase shifting is a fundamental control operation. A general approach to this operation, used extensively at both optical[12] and microwave[13] frequencies, is to alter the phase velocity along a fixed interval of a guiding medium. In this case, the phase shift per unit length is equal to the change in the propagation constant of the guided wave. One well-known method of altering the dispersion of millimeter waves is to introduce a plasma in the guiding medium. In their works Jacobs[2] and his coworkers have demonstrated that the phase shift can be accomplished by injecting plasma with PIN diodes[14]. Similar work at low frequency has been demonstrated very recently by Glance[15]. However, there are several shortcomings of PIN diode controlled millimeter-wave devices: (1) large phase shifts have not been achieved because of excess heating of the waveguide; (2) there are large losses (6 dB) due to excess metallization for contact to the junction region; and (3) the PIN diode becomes an integral part of the waveguide. This last shortcoming leads to complex boundary conditions and poor electrical isolation between the PIN diode and the waveguide structure. Inspired by previous work[2,14,15] we have come up with an elegant way of circumventing the difficulties associated with PIN diode control by using optical injection of plasma to illuminate the guide with above bandgap radiation, thereby creating the basic element of a new class of device --an optically controlled millimeter-wave device. Optical techniques offer the following advantages: (1) near perfect isolation, (2) low static and dynamic insertion losses, (3) fast response, (4) high power handling capability, (5) when picosecond pulses are used, it is possible for extremely high density plasmas to be injected without damaging the material.
(6) By proper choice of semiconducting material and laser wavelength one can generate plasma with any desirable density distributions and at any desirable time. (7) Ultrafast switching and gating of millimeter-wave signals are possible. (8) Using picosecond exciting-probing techniques, the dynamic evolution of the injected plasma can be studied in detail. Parameters related to

---

[2] H. Jacobs and M. M. Chrepta, "Electronic phase shifter for millimeter-wave semiconductor dielectric integrated circuits," IEEE Trans. Microwave Theory Tech, MTT-22 (1974), 411-417.
[10] J. C. Campbell and T. Li, "Electro-optic multimode waveguide switch," Appl. Phys. Lett. 33 (1978), 710-712.
[11] W. K. Burns, T. G. Giallorenzi, R. P. Moeller, and E. J. West, "Interferometric waveguide modulator with polarization independent operation," Appl. Phys. Lett. 33 (1978), 944-947.
[12] I. P. Kaminow, J. R. Carruthers, E. H. Turner, and L. W. Stulz, "Thin-film $LiNbO_3$ electro-optic light modulator," Appl. Phys. Lett. 22 (1973), 540-542.
[13] R. V. Garver, Microwave Diode Control Devices, Chapter 10, Artech House, Inc. (1976).
[14] B. J. Levin and G. G. Weidner, "Millimeter-wave phase shifters," RCA Rev. 34 (1973), 489-505.
[15] B. Glance, "A fast low loss microstrip p-i-n phase shifter," IEEE Trans. Microwave Theory Tech., MTT-27 (1979), 14-16.

transport properties of the carriers can be accurately determined.

Because of these apparent advantages, we feel that the optical techniques will not only enable us to characterize in detail the nature of wave-plasma interactions in the waveguide, but also provide practical ways for controlling millimeter waves. Furthermore, the characterization and modeling of the plasma layer on the millimeter-wave propagation in semiconducting waveguides will at least complement the work done by Jacobs et al[2] in understanding the nature of plasma-wave interaction. Recent development of mode-locked semiconductor lasers[14] and monolithic integration of an injection laser with a MESFET[16] further strengthen our belief that optical control of millimeter-waves is a viable technique.

Realizing this potential, we have initiated a research program, with internal support from the University of Maryland, College of Engineering (totaling $170,000) and external support from the Harry Diamond Laboratories ($70,000) and the National Science Foundation ($30,000 equipment grant) to investigate the effect of a light-induced plasma on the propagation of a millimeter wave in a semiconductor waveguide. The results include, besides the publications listed in the introduction, the presentation of a paper entitled, "Ultrafast optoelectronic modulation of millimeter-waves in GaAs waveguide" at the 12th International Quantum Electronics Conference in Munich, June 22-25, 1982.

We believe these efforts represent an important emergent field. Our work has led to the demonstration of a laser-controlled millimeter-wave phase shifter with phase shift up to 1400°/cm observed. In addition an ultrafast optoelectronic millimeter-wave modulator has been realized with modulation bandwidth well in excess of 1 GHz. More important, our work has enabled us to better understand the physics of these types of devices, including the PIN diode work done by Jacobs et al[2].

3. Technical Descriptions and Results

3.1 Concept of Optically Controllable Millimeter-Wave Propagation

Shown in figure 1 is a schematic of the optically controllable phase shifter. It consists of a rectangular semiconductor waveguide with tapered ends to allow efficient transition of millimeter-waves both to and from a conventional metal waveguide. Optical control is realized when the broad wall of the semiconductor guide is illuminated by light generated by either a proximal source or one removed by a suitable optical guiding medium. The width, a, and height, b, of the guide are selected so that it supports an E^y_{11} mode. The ini-

---

[2] H. Jacobs and M. M. Chrepta, "Electronic phase shifter for millimeter-wave semiconductor dielectric integrated circuits," IEEE Trans. Microwave Theory Tech, MTT-22 (1974), 411-417.

[12] I. P. Kaminow, J. R. Carruthers, E. H. Turner, and L. W. Stulz, "Thin-film $LiNbO_3$ electro-optic light modulator," Appl. Phys. Lett. 22 (1973), 540-542.

[16] P. T. Ho, L. A. Glasser, E. P. Ippen, and H. A. Haus, "Picosecond pulse generation with a cw GaAlAs laser diode," Appl. Phys. Lett., 33 (1978), 341-342.

tial depth of plasma injection is controlled by selecting an appropriate combination of optical radiation wavelength and semiconductor absorption properties.

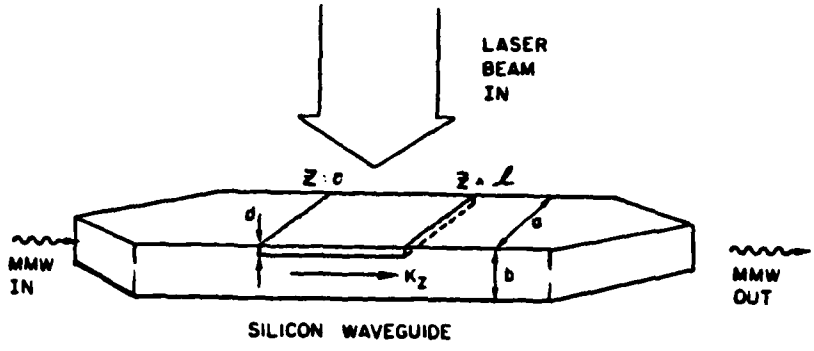

Fig. 1. Schematic diagram and operating principle of an optically controlled phase shifter. k_z is the propagation vector in the guide, d is the depth of the injected plasma layer, ℓ is the length of guide illuminated a and b are the width and height of the guide respectively.

At sufficiently small injection depths, the final thickness of the plasma is determined primarily by processes of carrier diffusion and recombination. The effect of plasma-occupied volume is to introduce a layer whose index at the millimeter-wave frequency is larger than the remaining volume of waveguide. From simple physical arguments one would expect this effect to become strong as one approaches and then exceeds the plasma density at which the value of the plasma frequency equals the frequency of the guided millimeter wave. At sufficiently high plasma densities, the millimeter wave is totally screened from the occupied volume, and one would expect that the phase shift per unit length would saturate as a function of plasma density. At extremely high densities, the plasma layer becomes metallic, and the dielectric waveguide becomes an image guide. As the optical illumination intensity increases from a low value, a significant phase shift will not appear until the plasma frequency exceeds the frequency of the guided millimeter wave after which it will rapidly rise and eventually saturate. However, the form and magnitude of the phase shift versus the intensity of illumination, and hence, the plasma density, depend in detail on the material and geometrical factors that characterize the optically perturbed guiding structure, and their determination requires a detailed solution of the corresponding boundary value problems. The optically induced phase shift $\Delta\phi$ for a given section of waveguide of length ℓ is determined by computing the propagation constant in the z direction first in the absence of the injected plasma, k_z, and then with the plasma, k_z' thus:

$$\Delta\phi = (k_z' - k_z)\ell \, . \qquad (1)$$

We have developed a complete theory and performed a computer calculation of the boundary value problem (see App. A) and have measured the phase shift as a function of laser intensity to test our model. Details of the experimental technique and numerical calculations are given in appendices A, B, and C. One of the typical results is shown in figure 2. The correspondence between the data and the theoretically predicted curve is quite good. We feel very confident that we have a good understanding of this problem. We observed a maximum phase shift of 59° at 94 GHz for a plasma column 1.6 mm long for a

waveguide of 2.4 x 1.0 mm^2 and 270° for a waveguide with 2 x 0.5 mm^2 cross-section, in good agreement with the theory. The maximum light energy used was about 10 μJ. In practical device applications, one is interested in the amount of phase shift per unit incident light energy. In the present case, the results indicate a phase shift per unit energy on the order of 25°/μj. By confining the plasma to a very thin layer and choosing a guiding structure close to cutoff, our calculations show a decrease in energy requirements for a given phase shift by at least two orders of magnitude, down to 2.5°/nJ.

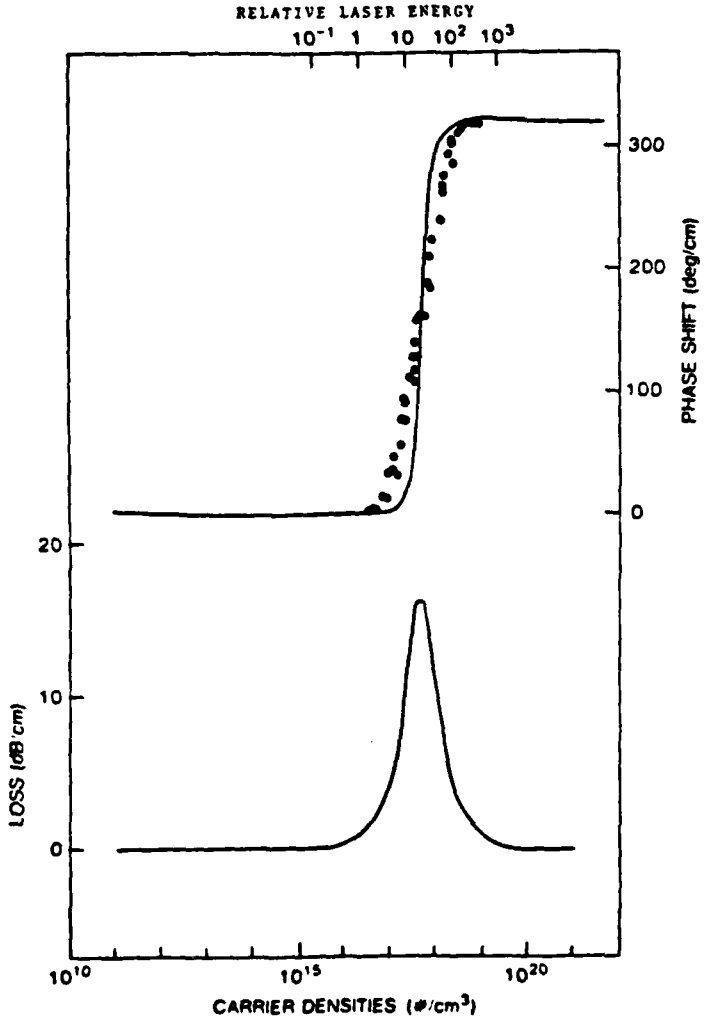

Fig. 2. Measured phase shift normalized to units of degree/cm. The scale for the upper abscissa applies to the reduced data points. The silicon waveguide has a cross-section of 2.4x1.0 mm^2.

By slight variations of the phase-shifting technique, we have also demonstrated optoelectronic switching, gating, and modulation of millimeter-wave

signal at 94 Ghz by an optically induced plasma in a silicon or GaAs waveguide[18,19,21]. A millimeter wave pulse width as short as 0.5 ns and variable to tens of nanoseconds can readily be obtained by this technique. We conclude from these studies that optical injection of plasma is superior to electrical injection because of its near-perfect isolation. The geometry and nature of the injected plasma column are more amenable to analysis. Excellent agreement between experiment and theory encourages further study and a search for a better experimental configuration to realize a new class of devices with high efficiency. Of particular interest is the development of an electronically steerable phased-array antenna.

3.2 Steady-State Analysis of Optically Controlled Millimeter-Wave Propagation in Dielectric Waveguide

In this project we have analyzed several different models that describe the millimeter-wave characteristics of a dielectric waveguide containing a plasma-dominated region. First we considered the case in which a plasma region of depth t_p was present over the entire broad wall of the dielectric guide; then we treated the plasma region as being infinitely thin and located only on the surface of the guide. For both of these cases we calculated the phase shift and attenuation resulting from the presence of the plasma. We are now in the process of describing the coupling between modes induced by the presence of the plasma.

The principle of the optically controllable phase shifter was discussed qualitatively in section 3.1. It was mentioned earlier in this section that the form and magnitude of the phase shift depends strongly on the material and geometrical factors that characterize the optically perturbed guiding structure. We have devised a model and carried out a detailed steady-state analysis of the general wave propagation problem in a dielectric waveguide with a plasma-occupied region. The results of these analyses are presented in appendix A. Here we just point out some of the main features.

We explain the calculated behavior of the phase shift and attenuation curves for the various modes in a 2.4 x 1.0 mm^2 silicon waveguide at 94 GHz as follows: As the plasma density increases from 10^{15} to 10^{20} cm^{-3} the skin depth at 94 GHz in silicon decreases from more than 200 μm to less than 1 μm. When the skin depth is equal to or larger than the plasma layer thickness, the millimeter wave penetrates deeply into the plasma layer, causing loss. The maximum loss occurs when the skin depth is about equal to the layer thickness. The higher order modes have more loss in this regime than the lower order modes because more of the wave power is concentrated in the plasma region when a higher order mode is propagating in the guide. As the plasma density increases further, the skin depth decreases. When the skin depth is less than the thickness of the plasma layer, the plasma region begins to act as a metallic

[18] C. H. Lee, S. Mak, and A. P. DeFonzo, "Millimeter-wave switching by optically generated plasma in silicon," Electron. Lett. 14 (1978), 733-734.
[19] C. H. Lee, "Picosecond optoelectronic switching in GaAs," appl. Phys. Lett, 30 (1977), 84-86.
[21] M. G. Li, W. L. Cao, V. K. Mathur, and Chi H. Lee, "Wide bandwidth, high-repetition rate optoelectronic modulation of millimeter-wave in GaAs waveguide," Electron. Lett. 18 (1982), 454-456.

conductor and the dielectric waveguide becomes an image line. The attenuation then drops off rapidly with increasing plasma density. The maximum phase shift of the higher order modes is also larger than that of the lower modes because the waveguide becomes more dispersive closer to cutoff.

The effect of varying the frequency of the millimeter wave in the 2.4 x 1.0 mm^2 guide for a 10-μm plasma depth is to shift the attenuation peak and the onset of the phase shift. This is to be expected since the skin depth is a decreasing function of frequency; therefore, the plasma density at which the greatest amount of interaction between the plasma and the wave occurs increases as the frequency is increased. Also, as the frequency is lowered, the maximum phase shifts and attenuations are larger. This is because the guide operates closer to cutoff at the lower frequencies.

When the same analysis is done for a GaAs waveguide, similar results are found. The general features of the phase shift and attenuation curves are the same as those for silicon; however, the curves are shifted toward lower plasma densities, consistent with the shift in the dielectric properties of GaAs versus Si.

Comparison of the results from the volume plasma model and the surface plasma model shows good agreement of the phase shifts and attenuations of the two models with respect to plasma density at small plasma depths.

As the thickness of the plasma layer gets larger, the agreement becomes poorer. Good agreement between the surface model and volume model with small plasma depth is very encouraging. Clearly, the simplicity of the surface model will aid us greatly in future analysis pertaining to mode conversion of a single incident wave.

Currently we are modelling the coupling between modes induced by the presence of the plasma by writing the fields in the plasma-controlled portion of the waveguide as a summation over the orthogonal set of modes which could propagate in the unperturbed guide.

3.3 Dynamic Bridge Method to Measure the Rapid Change of Phase and to Monitor the Carrier Decay Kinetics.

In the experiment on the ultrafast modulation of millimeter-wave signals by using Cr-doped GaAs waveguide, the pulsewidth of the modulated signals is usually narrower than the combined response time of the detector diode and oscilloscope. As a result, the convenient calibration technique employed in the Si waveguide work (see app. A) to obtain the values of phase shift and attenuation is not directly applicable here. We have, however, developed a dynamic bridge method to determine the values of the laser-induced phase shift and attenuation. This method exploits the fact that the temporal profile of the output of the bridge depends sensitively on (1) the initial phase angle between the electric fields in two arms of the bridge, (2) the laser-induced phase shift, and (3) the carrier decay dynamics and the dependence of the phase shift and attenuation of the millimeter wave on the carrier density. The dynamic range is very large in this method. We can follow the decay of carrier density over four orders of magnitude.

To understand how the dynamic bridge method works, let us consider a phasor diagram consisting of two interfering phasors representing the electric fields in the two arms of the bridge. Let E_A represent the electric field in the arm with dielectric waveguide (see fig. 3) and E_B, the rf field in the other arm. The output of the bridge is proportional to the resultant phasor. For simplicity, let us consider only the case where E_A and E_B are linearly polarized in the same direction. When the bridge is balanced before laser illumination, $E_A = -E_B$ and the output is zero. The situation in which the bridge is deliberately set to be unbalanced by an offset angle ϕ, is depicted in figure 4, where GA represents the resultant field E_R. It can be shown that

$$|E_R| = 2|E_B||\sin\frac{\phi}{2}|,$$

and if $|E_B|$ is normalized to unity,

$$|E_R| = 2|\sin\frac{\phi}{2}|.$$

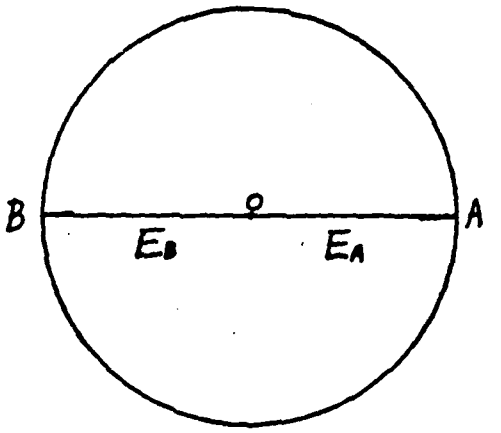

Figure 3. Phasor diagram consisting of two interfering phasors, E_A and E_B, representing electric fields in two arms of bridge.

The power detected by the diode is proportional to $2(1 - \cos\phi)$, as indicated in figure 5a. If the bridge inbalance is introduced by the laser pulse illumination, then the situation depicted in figure 5 still applies, except that ϕ now represents the-laser induced phase shift, ϕ_{laser}. After the laser pulse terminates, ϕ_{laser} changes from its maximum value to zero, according to the carrier decay kinetics and the relation between ϕ_{laser} and the carrier density. This relation has been calculated and is shown in appendices A and B. As ϕ_{laser} decreases, the phasor E_A rotates from its initial position OA along the circular arc ABCG to its equilibrium position OG. The resulting phasor describing the output of the bridge at a given instance is given by GB, GC, etc. figure 5c plots $|E_R|^2$ versus ϕ. However, $|E_R|^2$ versus time is more complicated. As we have mentioned earlier, $|E_R|^2$ depends on the functional forms of $\phi(N)$ and $N(t)$. On the other hand, knowing $\phi(N)$ and $N(t)$, one can calculate the temporal profile of the millimeter-wave signals. One example of such a calculation is given in figure 6a. The temporal profile of the resultant phasor shows a rich variety of forms depending on the following: (1) the initial offset phase angle ϕ_o between two phasors (set by adjusting the mechanical phase shifter), (2) the initial value of the laser-induced phase

shift and, (3) the carrier decay dynamics which determines the functional form of N(t), $\phi_{laser}(t)$, and $\alpha_{laser}(t)$, where $\alpha_{laser}(t)$ is the laser-induced attenuation coefficient of the millimeter waves. The qualitative temporal profiles of $|E_R^2|$ for $\phi_0 = \frac{\pi}{3}$ are shown in figure 7. The essential feature is the

appearance of the positive and negative portions of the signal. This characteristic results because the base-line of the $|E_R|^2$ plot is shifted when the bridge is

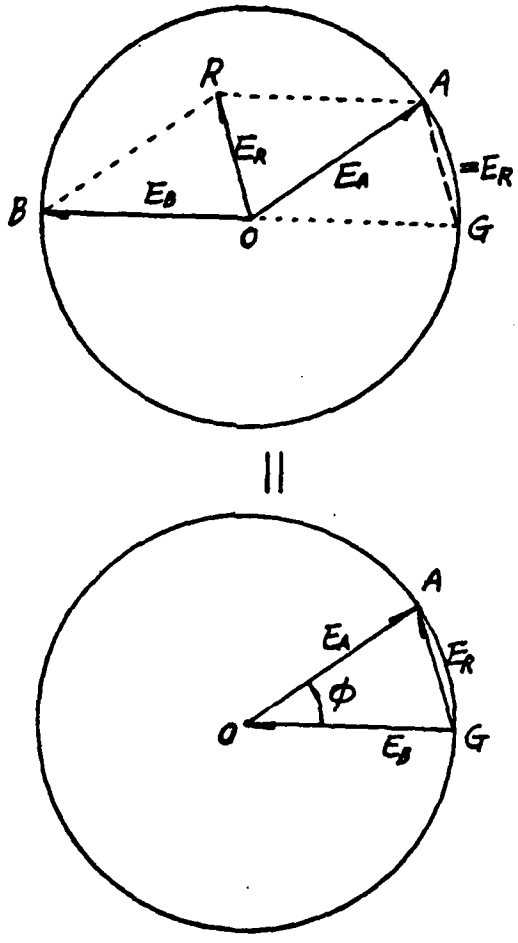

Figure 4. Phasor diagram for unbalanced bridge. Note simple geometric construction to obtain resultant phasor E_R, representing electric field at output of bridge.

initially set to be unbalanced. This is schematically shown in figure 7. When obtaining the final temporal profile one must also realize that the laser-induced loss can complicate the situation. Because of the variable loss, the phasor E_A will no longer rotate along a circle but rather along a complicated curve, since the magnitude of the phasor is also a function of time. This is shown in figure 8.

Fig. 5a

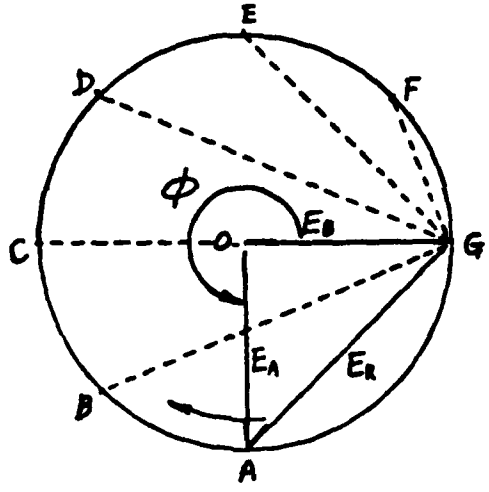

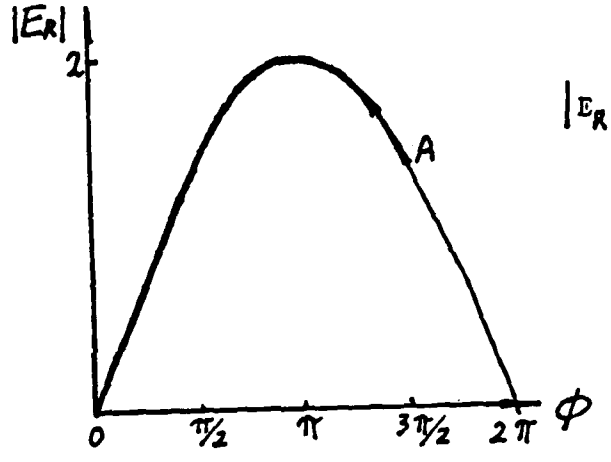

$$|E_R| = 2\left|\sin\frac{\phi}{2}\right|$$

Fig. 5b

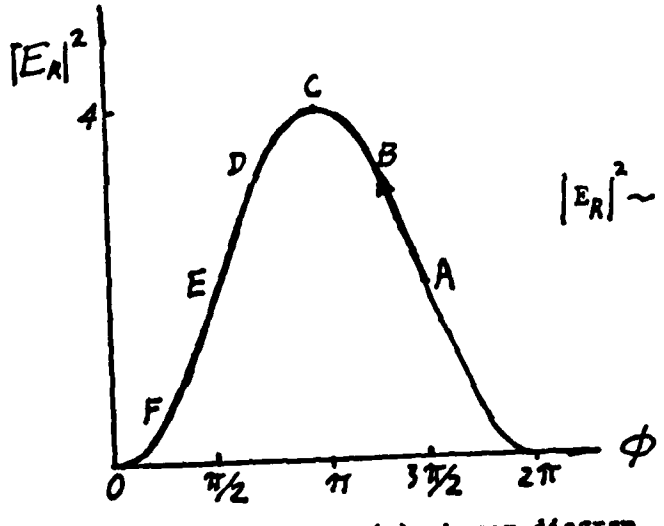

$$|E_R|^2 \sim 2(1-\cos\phi)$$

Fig. 5c

Figure 5. Balanced bridge case $\phi_o = 0$: (a) phasor diagram, (b) magnitude of E_R versus ϕ where phase angle between E_A and E_B is $\pi - \phi$, (c) $|E_R|^2$ versus ϕ.

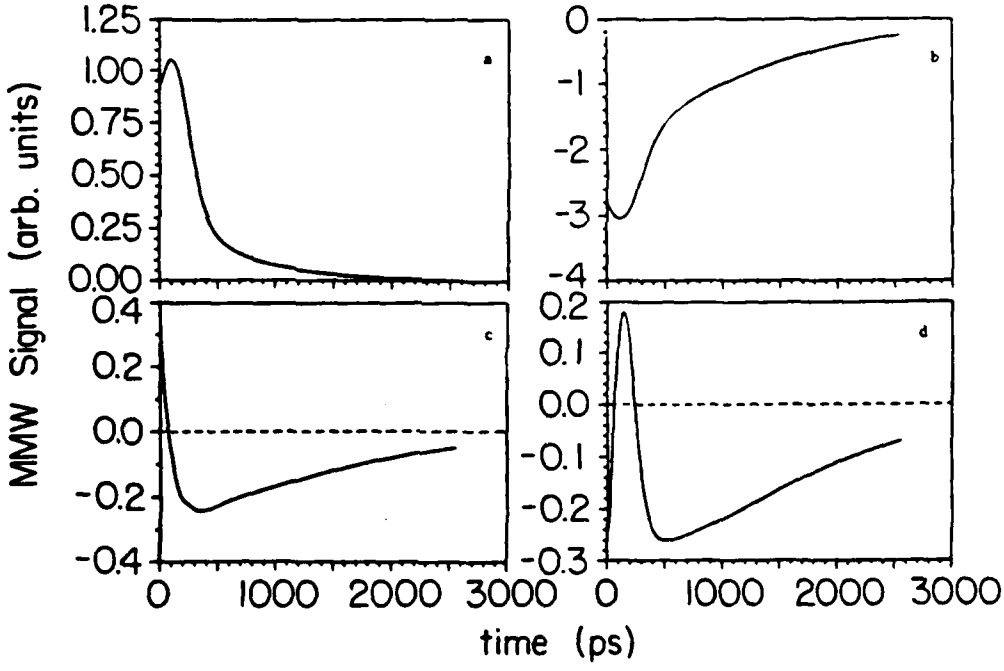

Figure 6. Theoretical temporal profile of the millimeter-wave signals generated for the unbalanced bridge due to the decay of the optically induced carriers. the curves are plotted for different initial phase angles between E_A and E_B. (a) 180°, the balanced case, (b) 0°, (c) 115° and (d) 235°.

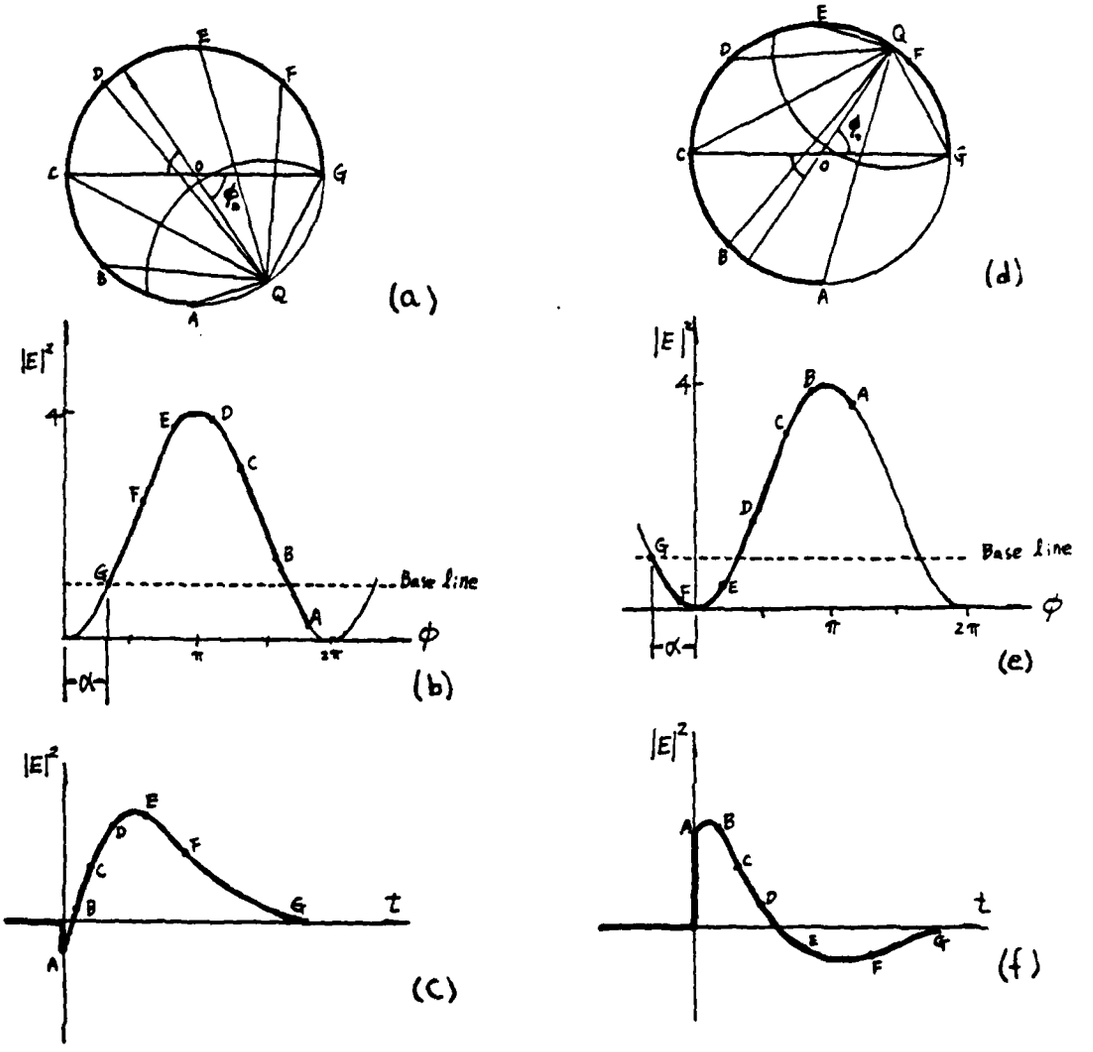

Figure 7. Qualitative temporal profile of $|E_R|^2$ (a) phasor diagram, (b) $|E_R|^2$ versus ϕ, (c) temporal profile of $|E_R|^2$ for initial phase angle between E_A and E_B equal to $\pi - \phi_0$, with $\phi_0 = -\frac{\pi}{3}$, (d), (e), (f) same as figure 7a, b, c with $\phi_0 = +\frac{\pi}{3}$

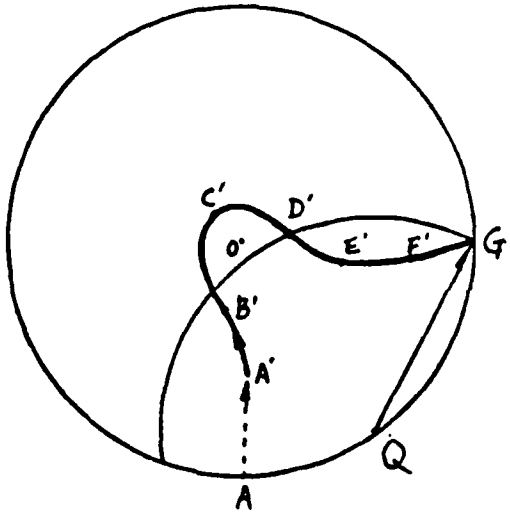

Figure 8. Decay path of laser-induced phasor OA when attentuation of phasor amplitude is taken into account. Phasor rotates with variable amplitude along path A'B'C'G.

Based on the theoretically calculated curves of phase shift and attenuation as a function of carrier density and assuming a certain decay characteristic of the excess carriers, we have calculated the temporal profile of the signal at the output of the detector. Figure 6 represents the results of these calculations with different initial phase angles between E_A and E_B for the Cr-doped GaAs waveguide at 94 Ghz. Here we have assumed a two component decay mechanism for the carriers with decay constants of τ_1 = 100 ps and τ_2 = 1000 ps. The mechanism for τ_1 is due to efficient recombination of carriers at chromium impurities, while that for τ_2 may be due to ambipolar diffusion. Figure 9 shows the observed millimeter-wave signals corresponding to the theoretical situation depicted in figure 6. In this particular case, a laser-induced phase shift of 270° was measured in good agreement with that predicted theoretically. In this measurement we can also follow the decay of carriers over a density range spanning four decades. With some refinement, this technique can also be applied to study carrier transport of more interesting cases, such as the temperature dependence of the transport parameters.

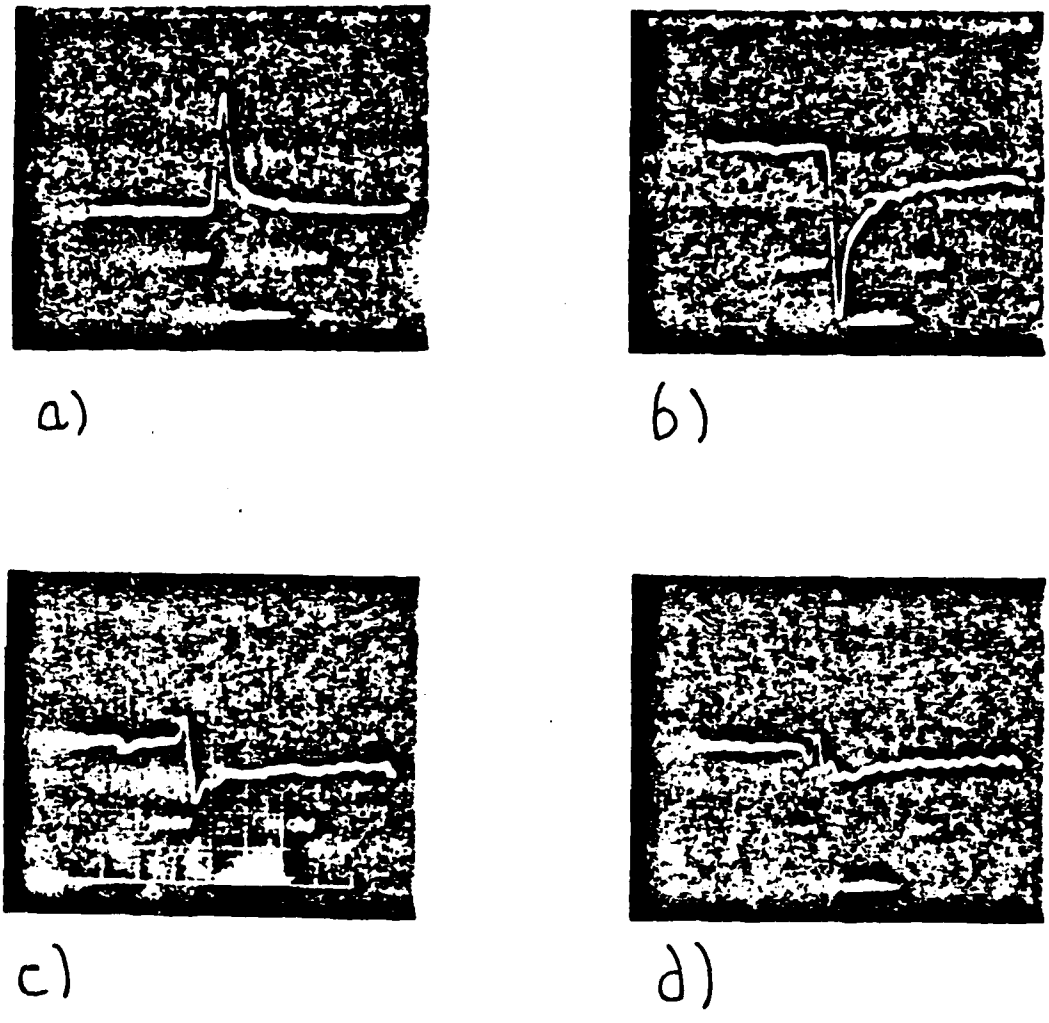

Figure 9. Experimentally observed millimeter-wave signals corresponding to theoretical ones in figure 6 in same cyclic order.

3.4 Highlights of Research Results

A phase shift of 1400°/cm of a 94-GHz millimeter-wave for a waveguide with dimensions close to cutoff (~0.5mm thick) has been observed accompanied by less than 1 dB of insertion loss. A theory has been developed to account in detail for the observed results. A computer code has been written to solve various boundary value problems, such as different thicknesses of the plasma layer, different modes, different frequencies, etc. Good agreement between theory and experiment gives us confidence to design devices based upon the computer calculations. Theoretical prediction shows that using a waveguide with dimensions close to cutoff, a phase shift of 2.5°/nJ of optical energy is possible.

Ultrafast millimeter wave switching without jitter has been demonstrated.

The switch response time is in the picosecond range. Millimeter-wave gating with picosecond precision has also been demonstrated and we have observed the shortest millimeter wave pulses ever reported (about 0.5 ns).

Using a Cr-doped GaAs waveguide, we have demonstrated a millimeter wave modulator with a bandwidth greater than 1 GHz. This device will be particularly attractive in pulse-coded communication applications, since the data rate can be extended well above 1 Gbit/s.

We have demonstrated for the first time the generation of 'chirped' millimeter wave pulses. This may be significant for pulse compression in coherent-pulse millimeter radar applications.

Finally, we have developed a dynamic bridge method to measure the dynamic phase shift induced by optical picosecond pulses and to monitor the decay kinetics of the carriers. The wide dynamic range of this method indicates that it is a sensitive technique to characterize the carrier transport parameters at low carrier density.

4. SUGESSTIONS FOR FUTURE RESEARCH TOPICS

4.1 Further Development of Dynamic Bridge Method

In section 3.3 we showed that the dynamic bridge method can determine the laser-pulse-induced phase shift which rises and decays rapidly on a sub-nanosecond time scale. In many instances, this method may be the only one for accurate measurement of the rapid phase shift. Further development of this technique to cover a large variety of situations should be carried out. The results of measurements obtained by this technique would be compared with those obtained by our earlier technique employed in our Si waveguide work[1] One can also apply the dynamic bridge method to study the carrier transport in different semiconducting materials, such as Si, Ge, and GaAs, and at different temperatures. For example, the carrier scattering time is related to temperature. We expect that these features may be detected by using the dynamic bridge method.

4.2 Laser-Controlled Phase-Shifter Research

We can continue to expand our research to investigate the influence of optically generated plasma on the propagation of millimeter waves in semiconductor waveguides. Our objectives thus far have been limited to (1) gaining an understanding of the physics of the plasma-wave interaction, (2) exposing any problems that may be associated with the devices in operation, and (3) devising a theoretical model that is amenable to computer analysis. So far, we have been quite successful in all three areas. Our goals for the next phase will be an in-depth and followup study. We will study the phase shifting effect with a waveguide close to cutoff. Our present studies show that in an oversize waveguide, the phase shift is 320°/cm, while in a waveguide with

[1] Chi H. Lee, P. S. Mak, and A. P. DeFonzo, "Optical control of millimeter-wave propagation in dielectric waveguides," IEEE J. Quantum Electron QE-16 (1980), 277-288.

thickness of 0.5 mm, a phase shift of 1500°/cm has been obtained. This indeed greatly relaxes the power requirement. The problem is mainly an engineering one, since there is a mismatch of cross-sectional area between the metallic and the dielectric waveguide. We will devote considerable effort to developing a launcher for smooth transition in coupling millimeter waves from a metallic waveguide to a dielectric one.

4.3 Mode Coupling in Optically Controlled Millimeter Wave Dielectric Waveguide.

As a demonstration of a practical phase-shifting device, we would like to use millimeter-wave devices to produce phase shifts of 180°, 90°, and 45°. A phase shift of 180° requires a length of 6 mm for the injected plasma column in an oversized waveguide. For waves propagating through a long dielectric section, the important problem of mode coupling effects must be addressed since it may not be possible to maintain the millimeter wave in the lowest order mode over a long distance. A good theoretical analysis and a detailed experimental characterization of the mode patterns and mode conversion and coupling are needed in order to properly design the phase shifting device. Mode coupling in integrated optics has been analyzed. The ideas and some of the results may be applied to the millimeter-wave range.

4.4 Ultrafast Switching, Gating, and Wide band Modulation of Millimeter-Wave Signals

For millimeter wave radar and high-data-rate communication, it is desirable to have a capability for ultrafast switching, gating and modulation. We have already demonstrated that switching and gating of millimeter waves with subnanosecond precision is attainable by laser controlled techniques[1] (see also app B). However, many important questions such as gain-bandwidth limitations, efficiency, minimum optical energy requirements, and maximum power-handling capability have not been considered. These questions can only be addressed meaningfully with a complete understanding of the millimeter-wave plasma interaction in the waveguide. For example, how does carrier diffusion and recombination affect wave propagation? By applying a fully developed dynamic bridge method, these questions may be answered. How does dielectric relaxation time affect the response time of the device? Is gating or switching best accomplished by injecting a surface plasma layer or a volume plasma? What are the best choices for laser and semiconducting material, etc? We will perform a systematic study to evaluate these parameters.

For wide bandwidth modulation one needs a semiconductor with an ultrafast carrier recombination time. In our early studies of optoelectronic switches[20], we have found that carriers in Cr-doped GaAs recombine in 50 ps.[20] This material is, therefore, a good candidate for a wide-band modulator. Either amplitude modulation of a transmitted wave in a single-arm waveguide or phase modulation in a two-arm millimeter-wave bridge arrangement can be

---

[1] Chi H. Lee, P. S. Mak, and A. P. DeFonzo, "Optical control of millimeter-wave propagation in dielectric waveguides," IEEE J. Quantum Electron QE-16 (1980), 277-288.

[20] C. H. Lee, A. Antonetti, and G. Mourou, "Measurements of the photoconductive lifetime of carriers in GaAs by optoelectronic gating techniques," Opt. Commun., 21 (1977), 158-161.

employed. Our most recent result based on the latter method is very encouraging. We have demonstrated the modulation of millimeter-wave signals at 94 GHz with a modulation bandwidth well in excess of 1 GHz. Based on the carrier lifetime data, the potential bandwidth should approach 10 GHz. A followup and in-depth study will be undertaken along this line. This device will be particularly attractive in pulse-coded communication as the data rate can be extended well above 1 Gbit/s.

Optoelectronic gating of millimeter-wave signals with picosecond precision offers many orders of improvement in signal to noise ratio in signal processing. This technological capability is necessary to reduce system vulnerability to electronic counter-measures. To explore these unique features we shall undertake an in-depth study with wide-bandwidth mixer diode/detectors.

4.5 Chirping of Millimeter-Wave Pulses and Coherent Pulse Compression

Using the modulation technique discussed in appendices B and C as well as in the last section, one generally obtains a well-defined pulse signal with good depth of modulation at the output of the bridge. The width of these pulses has been measured by a correlation technique frequently employed in the picosecond pulse work and found to be 600 ps, wider than the predicted pulsewidth by a factor of three. This discrepancy can be understood by realizing that the millimeter-wave pulse is generated by rapid phase modulation of the signal. As a result the pulse is actually chirped; i.e., there is a large frequency sweep within the pulse. Group velocity dispersion will broaden the 'chirped' millimeter-wave pulse as it propagates through a positively dispersive guiding structure, e.g., metallic waveguide, as observed in this case. It is interesting to point out that the millimeter-wave pulse can be as short as 200 ps, which contains only 20 cycles. If such a pulse is led to propagate through a negatively dispersive medium, it can further be compressed. We will search for a suitable material for such a demonstration. The compressed pulse will be very short. It is also interesting to find out how the compression process changes the signature of the original pulse. If the chirped rate is high enough and the compression ratio is large enough, the compressed pulse may have a carrier frequency characteristic that is quite different from that of the original pulse.

4.6 Development of Composite Dielectric Waveguide Structures

Although semiconducting materials used as waveguide media offer many advantages, materials costs will nevertheless be high. An alternative approach will be to use microwave ceramic materials such as alumina or magnesium titanate as the main body of the waveguide while overlaying a layer of semiconductor for control. This approach is particularly cost effective if a medium-range resistivity silicon can be used instead of high-purity silicon. According to figure 8-11 of Lee et al,[1] the loss and phase shift are insignificant until the plasma density reaches $10^{15}/cm^3$ for a plasma layer of 50-μm. This means that if one cements a silicon layer on an index matched ceramic waveguide, the resistivity of the silicon layer can be as low as 2 ohm-cm. This in turn means that the inexpensive silicon wafer can be used as the effective controlling element. Millimeter-wave propagation in such a composite

[1] Chi H. Lee, P. S. Mak, and A. P. DeFonzo, "Optical control of millimeter-wave propagation in dielectric waveguides," IEEE J. Quantum Electron QE-16 (1980), 277-288.

guiding structure with an optically injected plasma layer must be investigated. This structure may offer additional advantages in that the injected plasma will be confined to the semiconducting layer. The complicated transport phenomena encountered in bulk semiconductor devices may be avoided.

For another configuration, the composite dielectric waveguide structure may be sectionalized. In a region where only a normal guiding function is required, one uses the ceramic insular material, while in the region where some kind of control is needed, one uses semiconductor waveguide. These composite waveguide structures are essential for the realization of monolithic millimeter-wave integrated circuit technology.

4.7 Use of Diode Laser as Light Source

Up to now, we have been using the mode-locked Nd:YAG laser as the light source for controlling action. It is bulky. It may be quite adequate as a laboratory tool for investigation of the proposed research tasks but it is certainly not very practical for field operation. The ideal light source for such application should be compact and consume very little power. The diode lasers suit these requirements. According to our calculation, an optimally designed device should only require 1 nJ for 2.5° of phase shift. This energy requirement for the operation of the device is certainly available in most diode lasers. It is important to demonstrate the device operational principle by the use of diode lasers. We intend to include this in our investigation.

4.8 Study of Physics of Hot Carrier Transport in Semiconductors.

The prospect of ever larger scale integration of electronic circuits has increased the importance of the study of transport of carriers in semiconductors under high electric field. The transport of carriers under high electric field is usually characterized by its departure from Ohm's law, i.e., the current is a non linear function of the electric field. Among the many techniques for studying transport phenomena, we mention three which are relevant to our purpose:[21] (1) picosecond light pulse band-to-band excitation and probing of the excited carriers; (2) some combination of high dc or microwave field excitation and probing with a weak field; and (3) probing with a frequency source resonant with a time constant of interest, usually $\sim 10^{-12}$ s. We propose here to develop a technique which will combine some of the advantages offered separately by these three conventional methods. The transport of electrons under an electric field may be characterized by the complex conductivity, which is in turn determined by the carrier density and the various relaxation times. Optical methods can introduce a known number of carriers at a known initial energy (determined respectively by the intensity and frequency of the light), and energy redistribution of these electrons can be determined as a function of time to subpicosecond resolution by probing the band-to-band absorption of light. The change in the real part of the dielectric constant, however, requires an enormous carrier density (10^{19} cm^{-3} by rough estimates) because of the high optical frequency, 10^{15} Hz, compared with 10^{12} Hz carrier

[21] M. G. Li, W. L. Cao, V. K. Mathur, and Chi H. Lee, "Wide bandwidth, high-repetition rate optoelectronic modulation of millimeter-wave in GaAs waveguide," Electron. Lett. 18 (1982), 454-456.

response time. Lower frequency techniques (dc and microwave) measure the change in the complex conductivity but cannot yield direct information on the relaxation times because they are too fast; such information can only be obtained indirectly, by fitting experimental data to some theoretical calculations, for example. Direct examination at a resonant frequency (~10^{12} Hz) requires a frequency source at that range, a less-developed area.

The proposed technique exploits the available picosecond time resolution (and hence high frequency, 10^{12} Hz) from optical sources and the more sensitive measurements on the complex conductivity in low-frequency methods. The heart of the technique is a picosecond light pulse source, which can switch on and off, synchronously, square pulses of high dc voltage (up to kilovolt levels) and millimeter waves; the rising and falling edges of these square pulses are only limited by the optical pulse-width. The light pulse will be used to create a known carrier density by band-to-band absorption in a semiconductor sample. A square pulse of dc field, variable up to kilovolt levels will be used to excite the photogenerated carriers, and a square pulse of millimeter-wave will probe the complex conductivity of the sample as a function of both the dc field strength and the carrier density; thus, nonlinear effects due to high field and high carrier concentration can be detected. The sharp edges of the electric and millimeter-wave fields provide time resolution (i.e., high-frequency components are generated, up to over 10^{12} Hz) which may allow direct probing of the time constants, in the following manner. Suppose a square pulse of dc voltage is switched out sometime after the light pulse generates the carriers. A millimeter-wave pulse, with variable delay with respect to the dc pulse, will probe the complex dielectric constant n (Fig. 10). If the dc field rises faster than the carrier momentum relaxation time, different delay t_D' of the millimeter wave will lead to different values of the measured n. Similarly, different delay t_D between the light excitation pulse and the dc pulse will allow measurement of the energy redistribution time. The technique can be very sensitive by averaging the correlation measurements.

Since ever shorter available light pulse sources may be predicted 10^{-13} - 10^{-14} s resolution is not out of question. For a different project, we have available to us a cw 15-w argon laser to pump a mode-locked dye laser which has been shown to generate 0.09-ps pulses by colliding pulse mode-locking technique[23]. Should the output power be insufficient, we have available a Q-switched Nd:YAG laser which can be used to pump an amplifier for the dye; such an amplifier has been shown capable of amplifying very reliably 0.09 ps pulses up to gigawatt levels.[24]

At the beginning, however, to demonstrate the feasibility, we propose to use the existing facilities to make measurements in the 10 ps-region, cooling a suitable semiconductor sample to low temperature to lengthen the relaxation times.

---

[23] R. L. Fork, B. I. Greene, and C. V. Shank, "Generation of optical pulses shorter than 0.1 psec by colliding pulse model locking," Appl. Phys. Lett, 38 (1981), 671-672.

[24] R. L. Fork, C. V. Shank, and R. T. Yen, "Amplification of 70-fs optical pulses to gigawatt powers," Appl. Phys. Lett. 41 (1982), 223-225.

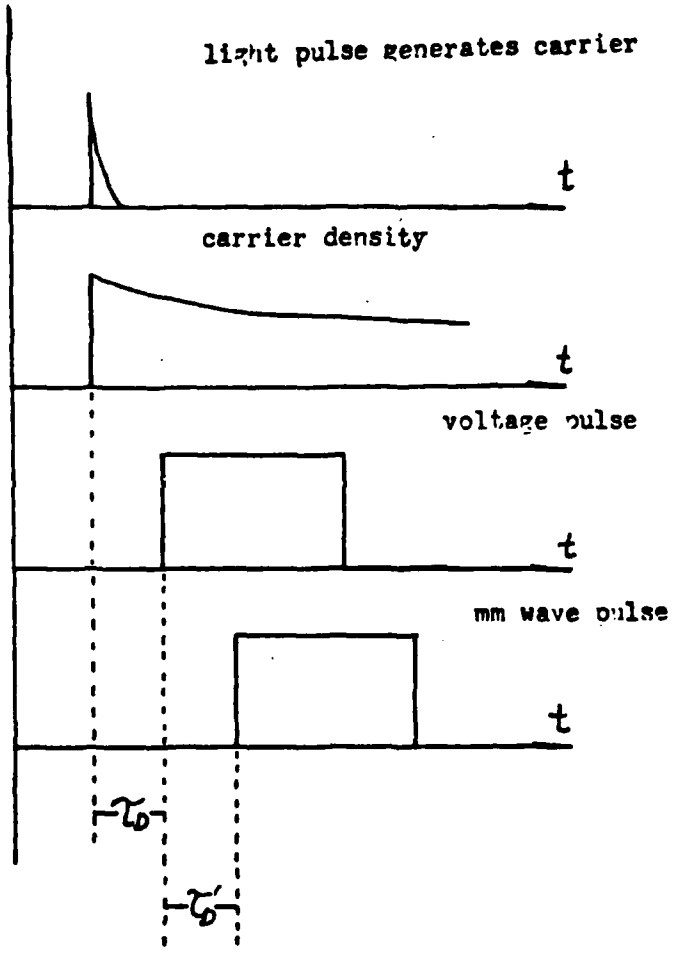

Figure 10. Relative timing of laser-induced solid-state plasma and dc and millimeter-wave pulses for characterization of hot carrier transports.

LITERATURE CITED

[1] Chi H. Lee, P. S. Mak, and A. P. DeFonzo, "Optical control of millimeter-wave propagation in dielectric waveguides," IEEE J. Quantum Electron QE-16 (1980), 277-288.

[2] H. Jacobs and M. M. Chrepta, "Electronic phase shifter for millimeter-wave semiconductor dielectric integrated circuits," IEEE Trans. Microwave Theory Tech, MTT-22 (1974), 411-417.

[3] W. J. Tomlinson, "Wavelength multiplexing in multimode optical fibres," Appl. Opt. 16 (1977), 2180-2194.

[4] M. Kobayashi and H. Herui, "Optical demultiplexer using coupling between nonidentical waveguides," Appl. Opt. 17 (1978), 3253-3258.

[5] J. Minowa, K. Aoyama, and Y. Fujii, "Silicon blazed-grating for low loss optical multiplexer," 1979 IEEE/OSA Conference on Laser Engineering and Applications, Digest of Technical Papers, paper 3.10 (1979), 54-55.

[6] K. E. Mortenson, A. L. Armstrong, J. M. Borrego, and J. F. White, "A review of bulk semiconductor microwave control components," Proc IEEE, 59 (1971), 1191-1200.

[7] K. L. Klohn, R. E. Horn, H. Jacobs, and E. Friebergs, "Silicon waveguide frequency scanning linear array antenna," IEEE Trans. Microwave Theory Tech., MTT-26 (1978), 764-773.

[8] J. A. Paul and Y. W. Chang, "Millimeter-wave image-guide integrated passive devices," IEEE Trans. Microwave Theory Tech., MTT-26 (1978), 751-754.

[9] I. P. Kaminow, "Optical waveguide modulators," IEEE Trans. Microwave Theory Tech., MTT-23 (1975), 57-70.

[10] J. C. Campbell and T. Li, "Electro-optic multimode waveguide switch," Appl. Phys. Lett. 33 (1978), 710-712.

[11] W. K. Burns, T. G. Giallorenzi, R. P. Moeller, and E. J. West, "Interferometric waveguide modulator with polarization independent operation," Appl. Phys. Lett. 33 (1978), 944-947.

[12] I. P. Kaminow, J. R. Carruthers, E. H. Turner, and L. W. Stulz, "Thin-film $LiNbO_3$ electro-optic light modulator," Appl. Phys. Lett. 22 (1973), 540-542.

[13] R. V. Garver, Microwave Diode Control Devices, Chapter 10, Artech House, Inc. (1976).

[14] B. J. Levin and G. G. Weidner, "Millimeter-wave phase shifters," RCA Rev. 34 (1973), 489-505.

[15] B. Glance, "A fast low loss microstrip p-i-n phase shifter," IEEE Trans. Microwave Theory Tech., MTT-27 (1979), 14-16.

[16] P. T. Ho, L. A. Glasser, E. P. Ippen, and H. A. Haus, "Picosecond pulse generation with a cw GaAlAs laser diode," Appl. Phys. Lett., 33 (1978), 341-342.

[17] I. Ury, K. Y. Lau, N. Bar-Chaim, and A. Yariv, "Very high frequency GaAlAs laser field-effect transistor monolithic integrated circuit," Appl. Phys. Lett. 41 (1982), 126-129.

[18] C. H. Lee, S. Mak, and A. P. DeFonzo, "Millimeter-wave switching by optically generated plasma in silicon," Electron. Lett. 14 (1978), 733-734.

[19] C. H. Lee, "Picosecond optoelectronic switching in GaAs," appl. Phys. Lett, 30 (1977), 84-86.

[20] C. H. Lee, A. Antonetti, and G. Mourou, "Measurements of the photoconductive lifetime of carriers in GaAs by optoelectronic gating techniques," Opt. Commun., 21 (1977), 158-161.

[21] M. G. Li, W. L. Cao, V. K. Mathur, and Chi H. Lee, "Wide bandwidth, high-repetition rate optoelectronic modulation of millimeter-wave in GaAs waveguide," Electron. Lett. 18 (1982), 454-456.

[22] For a more complete review, see Physics of Nonlinear Transport in Semiconductors, D. K. Ferry, J. R. Parker, and C. Jacoboni, ed., Plenum Press (1980), and Picosecond Phenomena II, R. M. Hochstrasser, W. Kaiser, and C. V. Shank, ed., Springer-Verlag (1980).

[23] R. L. Fork, B. I. Greene, and C. V. Shank, "Generation of optical pulses shorter than 0.1 psec by colliding pulse model locking," Appl. Phys. Lett, 38 (1981), 671-672.

[24] R. L. Fork, C. V. Shank, and R. T. Yen, "Amplification of 70-fs optical pulses to gigawatt powers," Appl. Phys. Lett. 41 (1982), 223-225.

DISTRIBUTION

Administrator
Defense Technical Information Center
ATTN: DTIC-DCA (12 copies)
Cameron Station, Building 5
Alexandria, VA 22314

U.S. Army Electronics Research & Development Command
ATTN: Commander, DRDEL-CG
ATTN: Technical Director, DRDEL-CT
ATTN: Public Affairs Office, DRDEL-IN
2800 Powder Mill Road
Adelphi, MD 20783

Commander
U.S. Army Missile Command
ATTN: DRSMI-RRO, Dr. G. A. Tanton
ATTN: DRDMI-TR, Dr. R. L. Hartman
ATTN: DRDMI-TB, Redstone Science Information Center
Redstone Arsenal, Alabama 35809

Commander
U.S. Army Electronics Command
ATTN: DRSEL-TL-IJ, Dr. H. Jacobs
Ft. Monmouth, NJ 07703

Commander
U.S. Army Communications-Electronics Command
ATTN: DRDCO-CON-RN-4, Dr. F. Schwering
Ft. Monmouth, NK 07703

Commander
U.S. Army Night Vision & Electro-Optics Laboratory
ATTN: DELNV-II, Dr. R. Shurtz
Ft. Belvoir, VA 22060

Commander
U.S. Army Research Office
ATTN: Dr. J. Mink
Research Triangle Park
Durham, NC 27709

Georgia Institute of Technology
Engineering Experiment Station
ATTN: J. J. Gallagher
ATTN: Dr. J. Wiltse
Atlanta, GA 30332

Commander
Naval Surface Weapons Center
ATTN: WR-43, Dr. A. Krall
Silver Spring, MD 20910

Massachusetts Institute of Technology
Francis Bitter National Magnet Laboratory
ATTN: Dr. K. J. Button
170 Albany Street
Cambridge, MA 02139

University of Illinois
Department of Electrical Engineering EERL-200
ATTN: Dr. P. D. Coleman
ATTN: Dr. T. A. Detemple
Urbana, IL 61801

Commander
Naval Research Laboratory
ATTN: Dr. V. L. Granatstein
Washington, D.C. 20375

Harry Diamond Laboratories
ATTN: Record Copy, 81200
ATTN: HDL Library, 81100 (3 copies)
ATTN: HDL Library, 81100 (Woodbridge)
ATTN: Technical Reports Branch, 81300
ATTN: Chairman, Editorial Committee
ATTN: Legal Office, 97000
ATTN: R. Bostak, 13300
ATTN: J. Sattler 13200
ATTN: J. Nemarich, 13300
ATTN: J. Silverstein, 13300
ATTN: H. Dropkin, 13200
ATTN: R. Leavitt, 13200
ATTN: G. Simonis, 13200
ATTN: M. Tobin, 13200
ATTN: D. Wortman, 13200
ATTN: R. Chase, 15300
ATTN: W. Trueheart, 11100
ATTN: D. Giglio, 15300
ATTN: A. Sindoris, 00211
2800 Powder Mill Road
Adelphi, MD 20783

APPENDIX A

Theory of Optically Controlled Millimeter-Wave Phase Shifters

AILEEN M. VAUCHER, CHARLES D. STRIFFLER, MEMBER, IEEE, AND CHI H. LEE, MEMBER, IEEE

Abstract—In this paper we analyze the millimeter-wave propagation characteristics of a dielectric waveguide containing a plasma-dominated region. Such a device presents a new method for controlling millimeter-wave propagation in semiconductor waveguides via either optical or electronic means resulting in ultrafast switching and gating. We have calculated the phase shift and attenuation resulting from the presence of the plasma. Higher order modes, both TE and TM, as well as millimeter-wave frequency variation, are studied in both Si and GaAs dielectric waveguides. We have also formulated a surface plasma model that is a good approximation to the more elaborate volume plasma model. Phase shifts are predicted to be as high as 1400°/cm for modes operating near cutoff. These modes suffer very little attenuation when the plasma region contains a sufficiently high carrier density.

I. INTRODUCTION

WE ARE CURRENTLY witnessing a resurgence of interest in millimeter-wave technology. The frequency band extending from 30 to 1000 GHz is attractive in several respects. Devices operating above *K*-band frequencies offer greater carrier bandwidth, better spatial resolution, and a more compact technology than presently used *X*- and *K*-band systems. Millimeter- and submillimeter-wave systems also have some advantages over optical systems, such as better atmospheric propagation in selected bands and a technology more amenable to frequency multiplexing [1]–[3], while retaining good angular resolution of the latter. A basic problem is how to effectively preserve these benefits. Our approach to the solution of this problem promises to yield much larger modulation bandwidths than are realizable with optical systems, while preserving the economy of the millimeter-wave system over a given carrier frequency band.

One of the important parts of the microwave and/or millimeter-wave system is the waveguide. At microwave frequencies, metal waveguides are commonly used. At higher frequencies, either microstrip or dielectric waveguide structures become more attractive. Microstrip transmission lines are used up to 30 GHz. For frequencies greater than 30 GHz, the losses in microstrip structures are high, and fabrication techniques become more difficult due to the small strip width and the substrate thickness. Dielectric rectangular waveguides become an alternative to the expensive metal waveguides. The use of high-purity semiconductor materials as dielectric waveguides is particularly important since active devices such as oscillators, Gunn or IMPATT diodes, mixers/detectors, and modulators can be fabricated monolithically with the semiconducting waveguides.

Manuscript received May 3, 1982; revised August 6, 1982. This work was supported in part by the Harry Diamond Laboratory; the U.S. Army; the Minta Martin Aeronautical Research Fund, College of Engineering, University of Maryland; and the University of Maryland Computer Science Facility.

The authors are with the Electrical Engineering Department, University of Maryland, College Park, MD 20742.

0018-9480/83/0200-0209$01.00 ©1983 IEEE

One important aspect of millimeter-wave devices is the control of the phase and amplitude of a wave propagating through the waveguide. The use of semiconductor bulk phenomena in implementing microwave control components has been discussed [4]. The principal phenomena explored have been the dielectric and conductive properties of the plasma state. A frequency-scanning millimeter-wave antenna utilizing periodic metallic-stripe perturbations on a silicon waveguide has been demonstrated [5]. Millimeter-wave dielectric image-guide integrated devices have been developed [6]. In the optical region, there are a variety of controllable waveguide devices which have not found their counterparts in the millimeter-wave region. High-speed light modulators that make use of the electrooptic, acoustooptic, and magnetooptic effects in bulk material have been described [7].

Phase shifting is a fundamental control operation. A general approach to this operation, used extensively at both optical [8] and microwave [9] frequencies, is to alter the phase velocity along a fixed interval of a guiding medium. In this case, the phase shift per unit length is equal to the change in the propagation constant of the guided wave. One well-known method of altering the dispersion of millimeter waves is to introduce a plasma into the guiding medium. In their work, Jacobs *et al.* [10] have demonstrated that the phase shift can be accomplished by injecting plasma with p-i-n diodes [11]. Similar work at low frequency has been demonstrated recently by Glance [12]. There are several shortcomings of p-i-n-diode-controlled millimeter-wave devices: a) large phase shifts have not been achieved due to excess heating of the waveguide; b) there are large losses (> 6dB) due to excess metallization for contact to the junction region; and c) the p-i-n diode becomes an integral part of the waveguide. This leads to complex boundary conditions and poor electrical isolation between the p-i-n diode and the waveguide structure.

Recently, we have demonstrated a way of circumventing the above difficulties. By illuminating the guide with above-bandgap radiation, we have created the basic element of a new class of device, an optically controlled millimeter-wave phase shifter and modulator. Optical control offers the following advantages: a) near perfect isolation; b) low static and dynamic insertion losses in some regimes; c) fast response; d) high power handling capability; e) when picosecond pulses are used, it is possible for extremely high density plasmas to be injected without damaging the material; f) by proper choice of semiconducting material and laser wavelength, one can generate plasma with any desirable density distributions and at any desirable time; g) ultrafast switching and gating of millimeter-wave signals is possible; and h) using picosecond exciting-probing techniques, the dynamic evolution of the injected plasma can be studied in detail. Parameters related to transport properties of the carriers can be accurately determined.

This paper analyzes in detail the changes that occur in the propagation characteristics of millimeter waves in a dielectric waveguide when a plasma-dominated region is present. The model and method analysis are presented in [13]. In that paper, both the experimental and theoretical studies concentrated primarily on the propagation of the dominant lowest order model (TM) denoted by $E^y_{1,1}$ for 94-GHz waves in a silicon waveguide. In practice, it has been found that for waves propagating in an over-sized waveguide with a plasma covered region, the waves will not remain in the fundamental mode. In this paper, we extend the analysis to include higher order TM modes $E^y_{p,q}$ and TE modes $E^x_{p,q}$. Calculations have also been carried out at frequencies other than 94 GHz. To understand the multimode propagation characteristics more fully, a model based on a surface plasma is devised, and the results compared with those obtained by a more elaborate calculation involving a finite thickness plasma layer. It is found that the surface plasma model gives a good approximation for plasma layers less than 10 μm in thickness. This is significant since we now have a simple theoretical model to predict the phase shift and to understand the mode-coupling mechanism in a general situation for plasma-controlled phase-shifting devices of arbitrary dimensions.

Recently, we have demonstrated the operation of a wide-bandwidth, high-repetition rate opto-electronic modulator for 94-GHz signals based on a plasma-controlled Cr-doped GaAs waveguide [14]. The rapid phase and amplitude modulation are achieved by using picosecond optical pulses to inject a plasma into the waveguide. In Cr-doped GaAs, in contrast to silicon, the electron-hole plasma recombines rapidly, i.e., in less than 100 ps, thus resulting in a high-speed, wide-bandwidth, and high-repetition rate operation of a millimeter-wave modulator. Therefore, in this paper, we extend our theoretical investigation of dielectric materials to include GaAs.

In Section II, the concept of a plasma-controlled dielectric waveguide is reviewed and earlier experimental results are summarized. The complete analysis, including the presentation of the surface plasma model, is then treated in Section III. It should be pointed out that the analysis presented here is quite general; it can be applied to the plasma-controlled dielectric waveguide devices no matter whether the plasma injection is by optical means, as in this work, or by electronic means, as in the work reported by Jacobs *et al.* [10].

II. Concept of Plasma-Controlled Dielectric Waveguide with Preliminary Experimental Results

Shown in Fig. 1 is a schematic of the optically controllable phase shifter. It consists of a rectangular semiconductor waveguide with tapered ends to allow efficient transition of millimeter waves both to and from a conventional metal waveguide. Optical control is realized when the broadwall of the semiconductor guide is illuminated by light generated by either a proximal source or one removed by a suitable optical guiding medium. The width a and height b of the guide are selected so that it supports an $E^y_{1,1}$ mode.

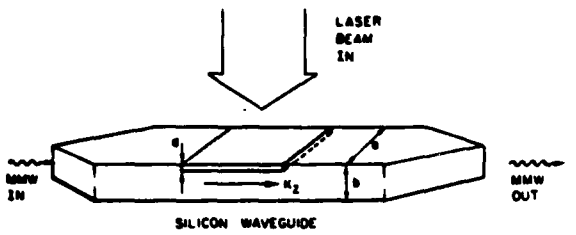

Fig. 1. Schematic diagram of the optically controlled phase shifter. The propagation vector in the guide is k_z, d is the depth of the injected plasma layer, a is the width of the guide, and b is the height of the guide.

The initial depth of plasma injection is controlled by selecting an appropriate combination of optical radiation wavelength and semiconductor absorption properties.

At sufficiently small injection depths, the final thickness of the plasma is determined primarily by processes of carrier diffusion and recombination. The effect of the plasma-occupied volume is to introduce a layer whose index of refraction at the millimeter-wave frequency is larger than that of the remaining volume of the waveguide. As the optical-illumination intensity increases from a low value, a significant phase shift will not appear until the plasma frequency exceeds the frequency of the guided millimeter wave, after which it will rapidly rise and eventually saturate. The form and magnitude of the phase shift versus the intensity of illumination, and hence the plasma density, depends in detail on the material and geometrical factors that characterize the optically perturbed guiding structure, and the determination of these quantities requires a detailed solution of the corresponding boundary value problems. The optically induced phase shift $\Delta\phi$ for a given section of waveguide of length l is determined by computing the propagation constant in the z direction; first, in the absence of the injected plasma k_z, and then with the plasma k_z'; thus, $\Delta\phi = (k_z' - k_z)l$.

Comparison between the experimental and the theoretical results presented in [13] and in Section III are shown in Fig. 2. The correspondence between the data and the theoretically predicted curve is excellent. As shown in Fig. 2, we observed a maximum phase shift of 59° at 94 GHz for a plasma column 1.6 mm in length with dynamic insertion loss of less than one decibel.

By slightly variations of the phase-shifting technique, we have also demonstrated opto-electronic switching and gating of millimeter-wave signals at 94 GHz by an optically induced plasma in a silicon waveguide [15]. A millimeter-wave pulse width as short as one nanosecond and variable to tens of nanoseconds can readily be obtained by this technique. We conclude from these studies that optical injection of plasma is superior to electrical injection because of its near-perfect isolation. The geometry and nature of the injected-plasma column are more amenable to analysis. Excellent agreement between experiment and theory encourages further study and a search for better experimental configurations to realize a new class of devices with high efficiency.

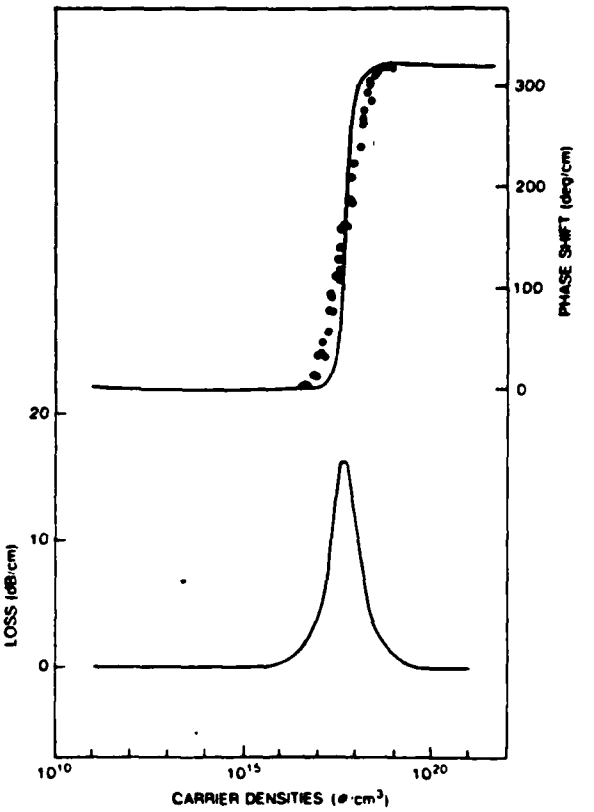

Fig. 2. Measured phase shift normalized to units of deg/cm [15].

III. Model and Analysis of a Plasma-Controlled Dielectric Waveguide

The geometry of the rectangular dielectric–plasma guide model is shown in Fig. 3. The guide cross section is in the $x-y$ plane, and the z coordinate represents the direction of propagation. The dimensions of the guide are denoted by a and b, and the plasma region thickness by t_p. The medium surrounding the waveguide is air. The relative dielectric constant and refractive index of the dielectric region $0 < y < b - t_p$ are ϵ_r and $n_r = \sqrt{\epsilon_r}$, respectively, and those of the dielectric–plasma region $b - t_p < y < b$ are [13]

$$\epsilon_p = n_p^2 = \epsilon_r - \alpha \frac{\omega_{pe}^2}{\omega^2 + \nu_e^2} - j\alpha \frac{\omega_{pe}^2}{\omega^2 + \nu_e^2} \frac{\nu_e}{\omega} \equiv (\eta - j\kappa)^2. \quad (1)$$

The free-charge contribution (plasma) is characterized by a plasma frequency $\omega_{pe} = (q_e^2 N_e / m_e \epsilon_0)^{1/2}$ of each species of density N_e, and an effective collision frequency ν_e. These various species in an optically formed plasma are denoted by thermally ionized and photo-induced holes (light and heavy) and electrons. The values of the various species properties, that is, density, effective mass, and collision frequency, are listed in Fig. 4(a) for Si and Fig. 4(b) for GaAs. In Fig. 4(a) the real part η and imaginary part κ of the refractive index for Si (see (1)) are plotted as a function

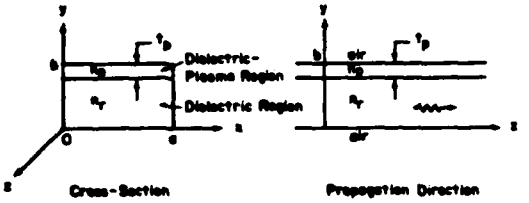

Fig. 3. Geometry of dielectric–plasma waveguide model.

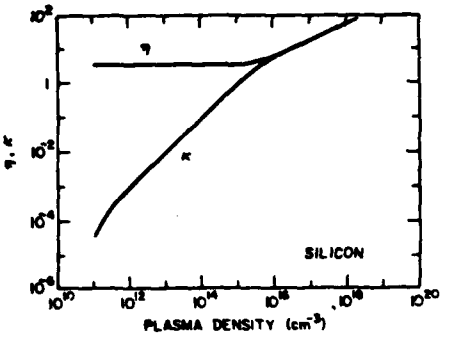

(a)

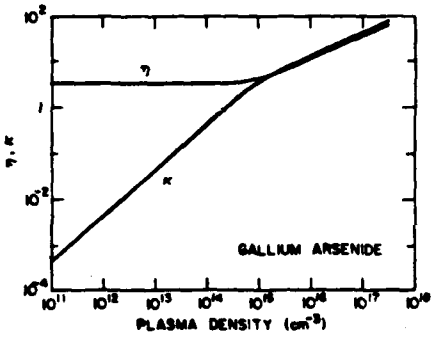

(b)

Fig. 4. (a) Plot of the plasma region refractive index versus plasma density in Si at 94 GHz. Here $P_L = 0.14\ N_p$; $P_H = 0.86\ N_p$; $m_e^* = 0.259\ m_0$; $m_p^* = 0.38\ m_0$; $m_{p_L}^* = 0.16\ m_0$; $m_{p_H}^* = 0.49\ m_0$; $\mu_e = 1500\ \text{cm}^2/\text{V}\cdot\text{s}$; $\tau_e = 2.2\times10^{-13}$ s; $\mu_h = 600\ \text{cm}^2/\text{V}\cdot\text{s}$; $\tau_p = 1.3\times10^{-13}$ s; and $N_{p0} = 10^{11}\ \text{cm}^{-3}$ [16], [17]. (b) Plot of the plasma-region refractive index versus plasma density in GaAs at 94 GHz. Here $P_L = 0$, $P_H = N_p$; $m_e^* = 0.06\ m_0$; $m_p^* = 0.5\ m_0$; $m_{p_H} = 0.8\ m_0$; $\mu_e = 8800\ \text{cm}^2/\text{V}\cdot\text{s}$; $\tau_e = 3.3\times10^{-13}$ s; $\mu_h = 450\ \text{cm}^2/\text{V}\cdot\text{s}$; $\tau_p = 1.28\times10^{-13}$ s; and $N_{p0} = 1.4\times10^6\ \text{cm}^{-3}$ [18–20].

of plasma density for a .94-GHz wave. Likewise, in Fig. 4(b) the refractive index in the plasma–dielectric region for GaAs is plotted. For each material, note the metallic nature of the plasma region for plasma density above about $10^{16}\ \text{cm}^{-3}$ for Si and $10^{15}\ \text{cm}^{-3}$ for GaAs.

For the case of well-guided modes, the analysis is considerably simplified in that the dispersion equation is essentially decoupled between the x and y directions [21]. That is, if the fields in the dielectric are assumed to vary as $\exp j(\omega t - k_x x - k_y y - k_z z)$, we find that boundary conditions in x determine k_x, those in y determine k_y, and from these one can then determine k_z. With these assumptions, the modes decouple into TM, called $E_{p,q}^y$, and TE, called $E_{p,q}^x$ modes. The propagation constant k_z is computed for the cases with and without the presence of the plasma region, k_z' (complex), k_z (real), respectively, and from these the plasma induced phase shift $\Delta\phi$ for a given length of waveguide l can be computed by

$$\Delta\phi = (\text{Re}\,k_z' - k_z)l, \text{ rad} \tag{2}$$

and the attenuation coefficient by

$$\alpha = \text{Im}\,k_z', \text{ cm}^{-1}. \tag{3}$$

Specifically, in a waveguide of dimensions a and b and with *no plasma present*, $n_p = n_r(\omega_{p_a} = 0)$, k_x and k_y for the $E_{p,q}^y$ mode are approximated by [21]

$$k_{x_{TM}} \simeq \frac{p\pi}{a}\left[1 + \frac{1}{\pi a}\frac{\lambda_0}{(\epsilon_r - 1)^{1/2}}\right]^{-1} \tag{4}$$

and

$$k_{y_{TM}} \simeq \frac{q\pi}{b}\left[1 + \frac{1}{\pi\epsilon_r b}\right]\frac{\lambda_0}{(\epsilon_r - 1)^{1/2}}^{-1}. \tag{5}$$

Here p is the number of extrema in the x direction, q is the number of extrema in the y direction, and λ_0 is the free-space wavelength of the propagating wave. Similarly, for well-guided $E_{p,q}^x$ modes, k_x and k_y are approximated by [21]

$$k_{x_{TE}} \simeq \frac{p\pi}{a}\left[1 + \frac{1}{\pi\epsilon_r a}\frac{\lambda_0}{(\epsilon_r - 1)^{1/2}}\right]^{-1} \tag{6}$$

and

$$k_{y_{TE}} \simeq \frac{q\pi}{b}\left[1 + \frac{1}{\pi b}\frac{\lambda_0}{(\epsilon_r - 1)^{1/2}}\right]^{-1}. \tag{7}$$

With these values of k_x and k_y, we can compute k_z in the guide without the plasma present

$$k_z = \left(n_r^2\frac{\omega^2}{c^2} - k_x^2 - k_y^2\right)^{1/2} \tag{8}$$

where k_x and k_y are given by either their TM values (4) and (5), or their TE values (6) and (7).

Now consider the case when the *plasma layer is present*, as shown in Fig. 3. Again, assuming the decoupling due to well-guided modes is valid, we note that the solutions for k_x for the $E_{p,q}^y$ and $E_{p,q}^x$ modes are given by (4) and (6). In the y direction, the solution for k_y for TM($E_{p,q}^y$) waves is found by solving [13]

$$\tan^{-1}\frac{K_d t_r}{k_r} + \tan^{-1}\left\{\frac{k_p}{k_r}\frac{\epsilon_r}{\epsilon_p}\tan\left[\tan^{-1}\left(\frac{K_d t_p}{k_p}\right) - k_p t_p\right]\right\} - k_r(b - t_p) + (q-1)\pi = 0 \tag{9}$$

and for TE($E_{p,q}^x$) waves

$$\tan^{-1}\frac{K_d}{k_r} + \tan^{-1}\left\{\frac{k_p}{k_r}\tan\left[\tan^{-1}\left(\frac{K_d}{k_p}\right) - k_p t_p\right]\right\} - k_r(b - t_p) + (q-1)\pi = 0. \tag{10}$$

In (9) and (10), we have defined the various k_y's in each

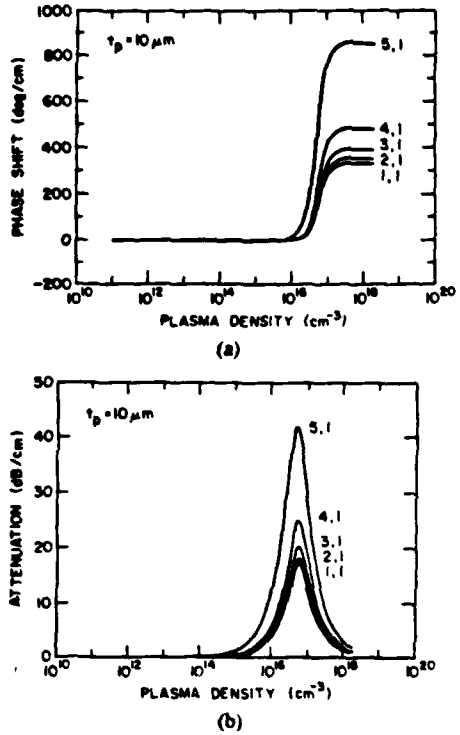

Fig. 5. (a) Phase-shift properties in a $2.4 \times 1\text{-mm}^2$ Si waveguide at 94 GHz with respect to plasma density for a plasma region thickness of 10 μm. Parametric dependence is the TM mode $E^y_{p,q}$. (b) Attenuation properties in a $2.4 \times 1\text{-mm}^2$ Si waveguide at 94 GHz with respect to plasma density for plasma region thickness of 10 μm. Parametric dependence is the TM mode $E^x_{p,q}$.

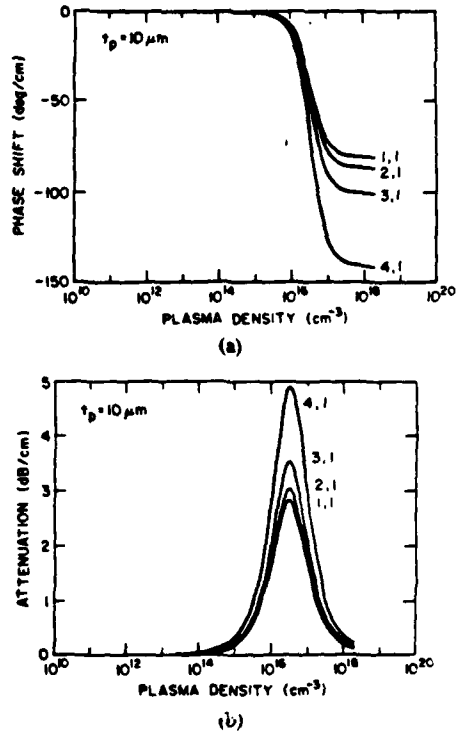

Fig. 6. (a) Phase shift properties in a $2.4 \times 1\text{-mm}^2$ Si waveguide at 94 GHz with respect to plasma density for a plasma region thickness of 10 μm. Parametric dependence is the TE mode $E^x_{p,q}$. (b) Attenuation properties in a $2.4 \times 1\text{-mm}^2$ Si waveguide at 94 GHz with respect to plasma density for a plasma region thickness of 10 μm. Parametric dependence is the TE mode $E^x_{p,q}$.

region (Fig. 3) as

$$K_a = \frac{2\pi}{\lambda_0}\left(n_\omega^2 - 1\right)^{1/2}$$

$$k_r = \frac{2\pi}{\lambda_0}\left(n_r^2 - n_\omega^2\right)^{1/2}$$

$$k_p = \frac{2\pi}{\lambda_0}\left(n_p^2 - n_\omega^2\right)^{1/2} \tag{11}$$

and n_ω is the effective refractive index of the wave in the decoupled guide. In the plasma layer, the index n_p is complex and depends upon the density of the plasma (see (1)). Substituting the k_y's into (9) and (10) results in transcendental equations for n_ω. These equations are solved numerically for n_ω, from which k_r is determined. The value of k_r is the value of k_y in the dielectric region in the presence of the plasma layer and thus k_z' may be found by

$$k_z' = \left(n_r^2 \frac{\omega^2}{c^2} - k_x^2 - k_r^2\right)^{1/2} \tag{12}$$

We can then compute the phase shift $\Delta\phi$ and attenuation α from (2) and (3), using (8) and (12).

In [15], plots of phase shift and attenuation versus plasma density, with plasma region thickness a parameter, were shown for the lowest order E^y mode, i.e., $E^y_{1,1}$. The Si waveguide cross sections for those plots were 2.4×1 mm^2 and 1×0.5 mm^2, and the plasma thickness was varied from 1 μm to half the guide depth. In this paper, we have calculated $\Delta\phi$ and α as a function of the plasma density for a rectangular Si waveguide of dimensions 2.4×1 mm^2 for all $E^y_{p,q}$ and $E^x_{p,q}$ modes that can propagate for a plasma region thickness of 10 μm. The results of the calculations are shown in Figs. 5 and 6. In Fig. 5(a) the phase shift per centimeter is plotted as a function of the plasma density for the $E^y_{1,1}$ through the $E^y_{3,1}$ modes, which are the only $E^y_{p,1}$ modes that can propagate in this guide. The corresponding loss in dB/cm is plotted in Fig. 5(b). As the plasma density increases from 10^{15} cm^{-3} to 10^{20} cm^{-3}, the skin depth in Si decreases from more than 200 μm to less than 1 μm. When the skin depth is equal to or larger than the plasma layer thickness, the millimeter wave penetrates deeply into the plasma layer causing loss. The maximum loss occurs when the skin depth is about equal to the layer thickness. The higher order modes have more loss in this regime than the lower order modes, because more of the wave power is concentrated in the plasma region when a higher order mode is propagating in the guide. As the plasma density increases further, the skin depth decreases. When the skin depth is less than the thickness of the plasma layer, the plasma region begins to act as a metallic conductor and the dielectric waveguide becomes an image line. The attenuation then drops off rapidly with increasing plasma density. The maximum phase shift of the higher order modes is also larger than that of the lower order modes because the

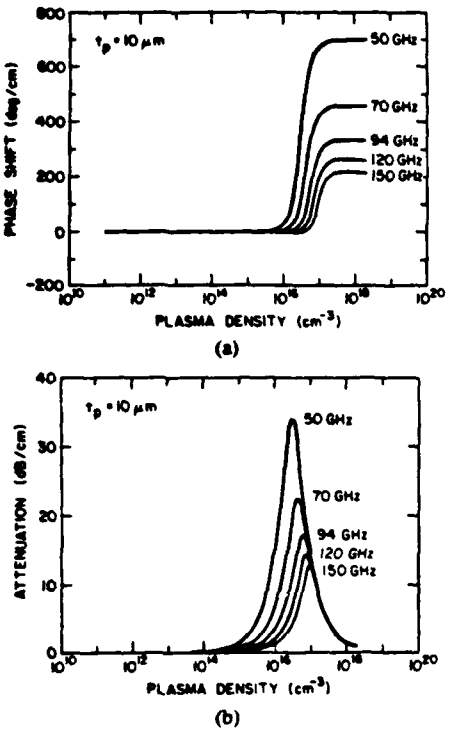

Fig. 7. (a) Phase-shift properties in a $2.4 \times 1\text{-mm}^2$ Si waveguide with respect to plasma density for a plasma-region thickness of 10 μm and the lowest order TM mode $E^y_{1,1}$. Parametric dependence is the frequency of the millimeter wave. (b) Attenuation properties in a $2.4 \times 1\text{-mm}^2$ Si waveguide with respect to plasma density for a plasma-region thickness of 10 μm and the lowest order TM mode $E^y_{1,1}$. Parametric dependence is the frequency of the millimeter wave.

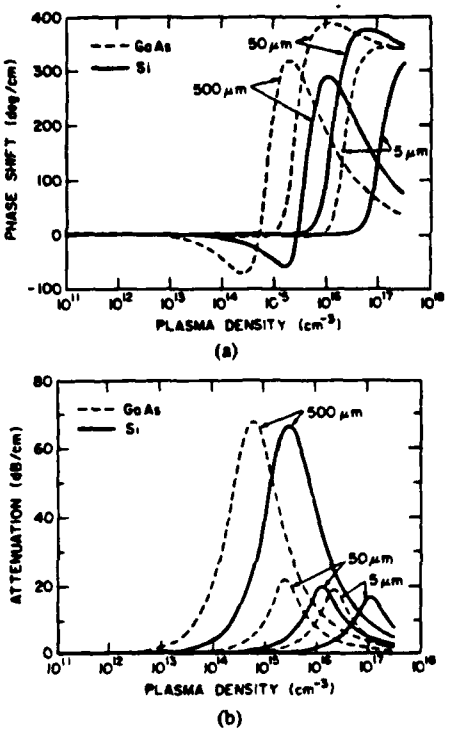

Fig. 8. (a) Comparison of the phase-shift characteristics of an $E^y_{1,1}$ mode propagating at 94 GHz in a $2.4 \times 1\text{-mm}^2$ waveguide for Si (solid lines) and GaAs (dashed lines) plotted with respect to plasma density. The three sets of curves correspond to plasma depths of 500 μm, 50 μm, and 5 μm, respectively. (b) Comparison of the attenuation characteristics of an $E^y_{1,1}$ mode propagating at 94 GHz in a $2.4 \times 1\text{-mm}^2$ waveguide for Si (solid lines) and GaAs (dashed lines) plotted with respect to plasma density. The three sets of curves correspond to plasma depths of 500 μm, and 50 μm, and 5 μm, respectively.

waveguide becomes more dispersive closer to cutoff. The other two TM modes this guide is capable of supporting at 94 GHz are the $E^y_{1,2}$ and $E^y_{2,2}$ modes, both of which are of higher order than the $E^y_{3,1}$ mode. Their maximum phase shifts are 1000°/cm and 1450°/cm, respectively.

Plots of the phase shift and attenuation curves for the TE modes, $E^x_{1,1}$ through $E^x_{4,1}$, in the $2.4 \times 1\text{-mm}^2$ guide at 94 GHz are shown in Fig. 6(a) and (b) for the 10-μm plasma layer. The results are similar to those found previously for the $E^y_{p,q}$ modes, except that the magnitude of the maximum phase shift is less and the maximum loss in the guide is less, reflecting the different field distribution requirements between the TE and TM modes.

The effect of varying the frequency of the millimeter wave in the $2.4 \times 1\text{-mm}^2$ guide for a 10-μm plasma depth is to shift the attenuation peak and the onset of the phase shift. This is shown in Fig. 7(a) and (b) for the $E^y_{1,1}$ wave. This is to be expected since the skin depth is a decreasing function of frequency; therefore, the plasma density at which the greatest amount of interaction between the plasma and the wave occurs increases as frequency is increased. Also, as the frequency is lowered, the maximum phase shifts and attenuations are larger. This is because the guide operates closer to cutoff at the lower frequencies. For a frequency of 50 GHz, only the mode shown, $E^y_{1,1}$, can propagate in the waveguide.

In Fig. 8(a) and (b), we have plotted the results for a $2.4 \times 1\text{-mm}^2$ GaAs waveguide. Because the features with respect to multimode and frequency variation are similar to those presented for Si, we have displayed only the lowest order TM mode $E^y_{1,1}$ results at 94 GHz with plasma thickness a parameter. For comparison, the Si guide results are displayed as solid curves. The general features of the GaAs curves are the same as those for Si; however, the curves are shifted toward lower plasma densities consistent with the shift in the dielectric properties of GaAs versus Si shown in Fig. 4.

A. Surface Model of the Plasma

A means of simplifying the calculation of the propagation constant k_x in the presence of the plasma is to assume that the plasma is located only at the surface with a surface plasma density

$$N_{s\alpha} = N_\alpha t_p, \text{ cm}^{-2} \tag{13}$$

where N_α is the volume density of each species α, and t_p is the thickness of the plasma. With this simplification, the plasma effect only appears in the boundary condition at $y = b$. A picture of this simplified model is shown in Fig. 9. The analysis proceeds as before by assuming that the solutions for k_x and k_y are decoupled. Again we find k_x is given by (4) and (6). We examine the plasma's reaction to

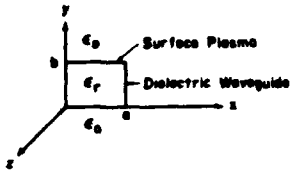

Fig. 9. Cross section of the plasma controlled dielectric waveguide with the plasma treated as a surface density.

the EM fields in terms of the linearized charge density ρ and a linearized current density $\vec{J}$, where

$$\rho = \sum_{\alpha} q_\alpha n_\alpha$$

$$\vec{J} = \sum_{\alpha} q_\alpha N_\alpha \vec{v}_\alpha. \tag{14}$$

Please note that N_α is the zeroth-order density of species α, and n_α represents the linearized response to the millimeter wave. Likewise, since the zeroth-order velocity of each species α is zero, $\vec{v}_\alpha$ represents the linearized velocity response to the millimeter wave. We use the integral form of Maxwell's Equations to find the boundary condition at $y = b$. The plasma quantities n_α and $\vec{v}_\alpha$ are found from the linearized fluid equations to be

$$n_\alpha = \frac{q_\alpha}{m_\alpha \omega} \frac{1}{\omega - i\nu_\alpha} \left\{ n_{\alpha 0} \left[\frac{\partial E_x}{\partial x} + \frac{\partial E_y}{\partial y} - ik_z E_z \right] + E_y \frac{\partial n_{\alpha 0}}{\partial y} \right\} \tag{15}$$

and

$$\vec{v}_\alpha = \frac{-iq_\alpha}{m_\alpha} \frac{\vec{E}}{\omega - i\nu_\alpha}. \tag{16}$$

We have defined $n_{\alpha 0} = N_{s\alpha}\delta(y - b)$, that is, a plasma located only at the surface $y = b$.

For TM waves, the surface plasma acts as a surface current and the transcendental equation for k_r becomes

$$\tan^{-1}\epsilon_r \frac{K_\alpha}{k_r} + \tan^{-1}\left\{ \epsilon_r \frac{K_\alpha}{k_r} \left[\frac{1}{1 - K_\alpha t_p(\epsilon_p - \epsilon_r)} \right] \right\} - k_r b + (q-1)\pi = 0 \tag{17}$$

where K_α and k_r are as in (11). For TE waves, the surface plasma acts as a surface charge and the transcendental equation for k_r becomes

$$\tan^{-1}\frac{K_\alpha}{k_r} + \tan^{-1}\left\{ \frac{K_\alpha}{k_r} \left[1 + \left(\frac{2\pi}{\lambda_0} \right)^2 \frac{t_p}{K_\alpha}(\epsilon_p - \epsilon_r) \right] \right\} - k_r b + (q-1)\pi = 0. \tag{18}$$

While (17) and (18) are still transcendental, their solutions are much simpler than those of (9) and (10). Fig. 10(a) and (b) shows the results of the surface plasma model analysis in comparison to the volume model presented in the previous figures. Good agreement of the phase shifts and attenuations of the two models with respect to plasma density at small plasma depth for a TM wave at 94 GHz is seen. As the thickness of the plasma layer gets larger, the agreement becomes poorer, as expected. Similar agreement is found for the TE waves and for higher order modes of both the TE and TM waves. Clearly, the simplicity of this model will aid us in figure analysis pertaining to mode conversion of a single incident wave.

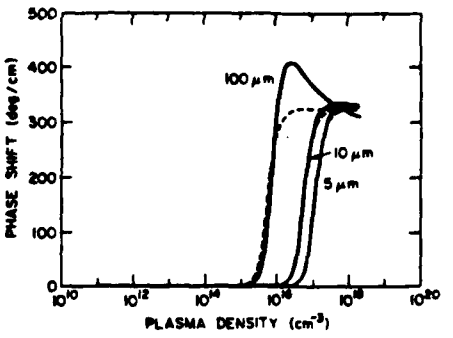

(a)

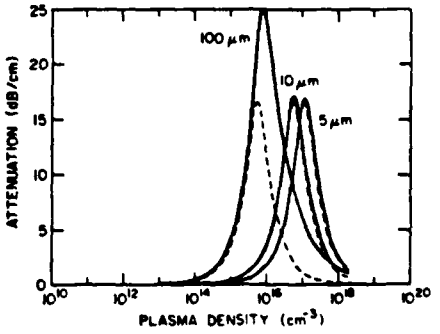

(b)

Fig. 10. (a) Comparison of the phase-shift characteristics of an E_{11}^{y} mode propagating at 94 GHz in a 2.4 × 1-mm² Si waveguide for the surface model (dashed lines) and the volume model (solid lines) plotted with respect to plasma density. The three sets of curves correspond to plasma depths of 100 μm, 10 μm, and 5μm, respectively. (b) Comparison of the attenuation characteristics of an E_{11}^{y} mode propagating at 94 GHz in a 2.4 × 1-mm² Si waveguide for the surface model (dashed lines) and the volume model (solid lines) plotted with respect to plasma density. The three sets of curves correspond to plasma depths of 100 μm, 10 μm, and 5 μm, respectively.

IV. Conclusion

We have analyzed in detail the steady-state millimeter-wave propagation characteristics of Si and GaAs dielectric waveguides that contain a plasma-dominated region. We have calculated the phase shift and attenuation properties resulting from the presence of the plasma. Higher order modes were examined as well as frequency variation of the millimeter wave for all modes capable of propagating in a given sized guide. A surface plasma model was formulated that greatly simplified the analysis, yet gave good agreement with the more elaborate volume model. This model will facilitate the computation of a more complicated situation where mode coupling effects may be important. Phase shifts as high as 1400°/cm are predicted for modes near cutoff. This analysis indicates that in an oversized guide where many modes can be present, the properties of all modes are similar in both their expected phase shift as well as their attenuation properties.

REFERENCES

[1] W. J. Tomlinson, "Wavelength multiplexing in multimode optical fibers," *Appl. Opt.*, vol. 16, pp. 2180–2194, 1977.

[2] M. Kobayashi and H. Terui, "Optical demultiplexer using coupling between nonidentical waveguides," *Appl. Opt.*, vol. 17, pp. 3253–3258, 1978.

[3] J. Minowa, K. Aoyama, and Y. Fujii, "Silicon blazed-grating for low loss optical multiplexer," in *Dig. Tech. Papers, 1979 IEEE/OSA Conf. on Laser Engineering and Applications*, paper 8.10, pp. 54–55.

[4] K. E. Mortenson, A. L. Armstrong, J. M. Borrego, and J. F. White, "A review of bulk semiconductor microwave control components," *Proc. IEEE*, vol. 59, pp. 1191–1200, 1971.

[5] K. L. Klohn, R. E. Horn, H. Jacobs, and E. Friedbergs, "Silicon waveguide frequency scanning linear array antenna," *IEEE Trans. Microwave Theory Tech.*, vol. MTT-26, pp. 764–773, 1978.

[6] J. A. Paul and Y. W. Chang, "Millimeter-wave image-guide integrated passive devices," *IEEE Trans. Microwave Theory Tech.*, vol. MTT-26, pp.751–754, 1978.

[7] I. P. Kaminow, "Optical waveguide modulators," *IEEE Trans. Microwave Theory Tech.*, vol. MTT-23, pp. 57–70, 1975.

[8] I. P. Kaminow, J. R. Carruthers, E. H. Turner, and L. W. Stulz, "Thin-film $LiNbO_3$ electro-optic light modulator," *Appl. Phys. Lett.*, vol. 22, pp. 540–542, 1973.

[9] R. V. Garver, *Microwave Diode Control Devices*. Dedham, MA: Artech House, 1976, ch. 10.

[10] H. Jacobs and M. M. Chrepta, "Electronic phase shifter for millimeter-wave semiconductor dielectric integrated circuits," *IEEE Trans. Microwave Theory Tech.*, vol. MTT-22, pp. 411–417, 1974.

[11] B. J. Levin and G. G. Wiedner, "Millimeter-wave phase shifters," *RCA Rev.*, vol. 34, pp. 489–505, 1973.

[12] B Glance, "A fast low loss microstrip p-i-n phase shifter," *IEEE Trans. Microwave Theory Tech.*, vol. MTT-27, pp. 14–16, 1979.

[13] Chi H. Lee, Paul S. Mak, and A. P. DeFonzo, "Optical control of millimeter-wave propagation in dielectric waveguides," *IEEE J. Quantum Electron.*, vol. QE-16, pp. 277–288, 1980.

[14] M. G. Li, W. L. Cao, V. K. Mathur, and C. H. Lee, "Wide bandwidth high-repetition rate optoelectronic modulation of millimeter waves in GaAs waveguide," *Electron. Lett.*, vol. 14, pp. 454–456, 1982.

[15] Chi H. Lee, Paul S. Mak, and A. P. DeFonzo, "Millimeter-wave switching by optically generated plasma in silicon," *Electron. Lett.*, vol. 14, pp. 733–734, 1978.

[16] R. A. Smith, *Semiconductors*. Cambridge, MA: Cambridge, 1968, pp. 100 and 347.

[17] B. Lax and J. G. Mavorides, "Statistics and galvano-magnetic effects in germanium and silicon with warped energy surfaces," *Phys. Rev.*, vol. 100, pp. 1650–1657, 1955.

[18] *The Merck Index*, M. Windholz, Ed., 9th ed. Rahway, NJ: Merck, p. 561, 1976.

[19] *CRC Handbook of Chemistry and Physics*, R. C. Weast, Ed., 49th ed. Cleveland, OH: Chemical Rubber Company, 1968–1969, pp. E98–E102.

[20] C. O Thurmond, "The standard thermodynamic function of the formation of electrons and holes in Ge, Si, GaAs, and GaP," *J. Electrochem. Soc.*, vol. 122, p. 1133, 1975.

[21] E. A. J. Marcatili, "Dielectric rectangular waveguide and direction coupler for integrated optics," *Bell Syst. Tech. J.*, vol. 48, p. 2103, 1969.

Charles D. Striffler (M'77) received the B.S. degree in science engineering and the M.S. and Ph.D. degrees in nuclear engineering at the University of Michigan in 1961, 1963, and 1972, respectively.

He was at Knolls Atomic Power Laboratory from 1965 to 1967, the Naval Research Laboratory from 1972 to 1975, and the University of Maryland since 1974, where he is an Associate Professor in Electrical Engineering. His areas of research in the plasma physics field are high-power microwave generation from rotating *E*-layers, collective ion acceleration using intense *E*-beams, and plasma millimeter-wave interactions in dielectric waveguides.

Aileen M. Vaucher was born in St. Paul, MN, in 1956. She received the B.S. degree in electrical engineering from the University of Minnesota, in 1979, and the M.S. degree from the University of Maryland, College Park, in 1980. She is currently working towards the Ph.D. degree in the field of electrophysics at the University of Maryland.

Her research interests are bulk GaAs lasers and plasma millimeter-wave interactions in dielectric waveguides.

Chi H. Lee (M'79) received the B.S. degree in electrical engineering from the National Taiwan University, Taipei, Taiwan, and the M.S. and Ph.D. degrees in applied physics from Harvard University, Cambridge, MA, in 1959, 1962, and 1968, respectively.

He was with the IBM San Jose Research Laboratory from 1967 to 1968. Since 1968 he has been with the University of Maryland, College Park, where he is now a Professor of Electrical Engineering. His areas of research include picosecond phenomena, nonlinear optical effects, and millimeter-wave devices.

Dr. Lee is a member of Sigma Xi and the American Physical Society.

APPENDIX B

WIDE BANDWIDTH, HIGH-REPETITION-RATE OPTOELECTRONIC MODULATION OF MILLIMETRE WAVES IN GaAs WAVEGUIDE

Indexing terms: Optoelectronics, Dielectric waveguides, Laser-beam applications

The generation of ultrashort, chirped and coherent millimetre-wave pulses by an optical method is reported. Using this technique, the modulation of millimetre-wave signals at 94 GHz with a modulation bandwidth in excess of 1 GHz is readily achievable.

Optically controlled microwave or millimetre-wave devices have been a topic of great interest recently. Utilising a laser-induced electron-hole plasma in semiconductors to control the propagation of RF signal, previously,[1] we have successfully demonstrated the switching, gating and phase shifting of millimetre-wave signals in Si-waveguides with picosecond precision. Phase shifts as large as 300°/cm at 94 GHz were observed. In the experiment involving the switching and gating of RF waves, millimetre-wave pulses with pulsewidths as short as 1 ns and variable to tens of nanoseconds have also been generated. In these earlier experiments,[2] high-resistivity Si was used as the waveguide material. Since carrier lifetime in pure silicon is in the millisecond range, for generating short RF pulses, one generally requires two separate laser pulses, one to 'turn on' and the other to 'turn off' the millimetre-wave signal. Furthermore, the repetition rate of the device is limited by the carrier recombination rate to less than 10 kHz. In this letter,

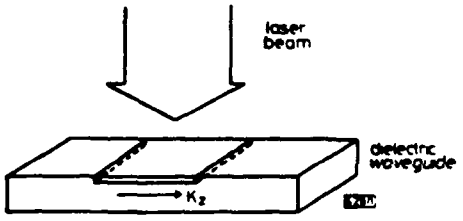

Fig. 1 *Schematic diagram of an optically controlled phase shifter*
K_z is propagation vector in waveguide

we will report on our most recent study of this type of device using Cr-doped GaAs as the waveguiding medium. Owing to rapid carrier recombination,[3] only a single picosecond optical pulse is needed to produce ultrashort millimetre-wave pulses. This feature has been utilised to construct a high-speed millimetre-wave modulator with a repetition rate well in excess of 1 GHz.

The optical control of RF-waves offers the following advantages:

(*a*) near-perfect isolation between the controlling and the controlled devices
(*b*) low static and dynamic insertion losses
(*c*) the possibility of producing fast responses with picosecond precision
(*d*) a high power handling capability.

The basic principle of optical control of millimetre waves is illustrated schematically in Fig. 1. The propagation constant K_z in an interval ΔL of a rectangular GaAs waveguide (2·4 × 1·0 mm) is changed to K_z' by illuminating the broadwall with optical radiation. The absorbed light generates an electron-hole plasma resulting in a change of the complex index of refraction of the semiconductor thereby altering the boundary conditions of the waveguide and changing the propagation constant. A millimetre wave launched into the waveguide experiences amplitude and/or phase modulation while propagating through the illuminated interval. The ratio of amplitude to phase modulation depends on the density and geometry of the plasma. For example, if the density yields a skin depth δ much less than the thickness of the plasma layer, the effect of the plasma is equivalent to an image guide. This results primarily in a phase shift ϕ, given by the relationship

$$\phi = (k_z - k_z')\,\Delta L$$

In the general case, the transient response of the device depends on the transport parameters of the optically induced carriers, such as the carrier collision time, mobility, diffusion characteristics etc. The mechanism for phase shift and attenuation can then be approximately described in terms of a model, developed during the study, based on Marcatili's approximation.[4]

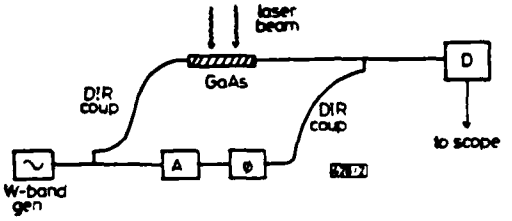

Fig. 2 *Experimental arrangement for generating 'chirped' millimetre-wave pulses*

The experimental arrangement is depicted in Fig. 2. A millimetre-wave bridge similar to that used by Jacobs and Chrepta[5] was employed. A GaAs guide was inserted in one arm of the bridge. The dielectric waveguide was composed of a 25 mm-long GaAs slab with a cross-section of 2·4 × 1·0 mm², which was considered to be an oversized waveguide for the 94 GHz signals. The ends of the slab were tapered for transitions with minimum reflection from standard W-band

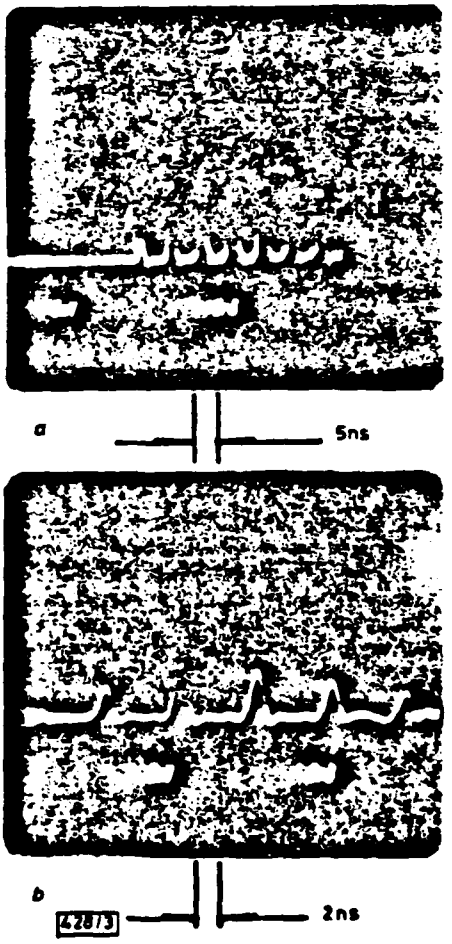

Fig. 3 *Millimetre-wave pulse train mimicking the incident optical pulse train*

Different time scales are shown in (*a*) and (*b*), respectively. Individual pulse in train is 'chirped' and its duration is measured by a correlation technique to be about 600 ps

waveguide operating in a TE_{10}-mode to dielectric waveguide. The dark resistivity of the Cr-doped GaAs was 10^7 Ωcm. Initially, without laser pulse illumination of the GaAs waveguide, the bridge was balanced by adjusting the variable attenuator A and mechanical phase shifter ϕ in the other arm so that there was no signal at the output. When a single 0·53 μm pulse of about 20 μJ and 30 ps duration extracted from a frequency doubled mode-locked Nd YAG laser illuminated the GaAs waveguide, a high-density electron-hole plasma was generated on the surface of the GaAs slab, causing a phase shift in the millimetre-wave signal as it propagated through the plasma covered region of the waveguide. The bridge became unbalanced and a signal appeared at the output of the bridge. This signal would persist until the excess carriers recombined. As the lifetime of the excess carrier is of the order of 100 ps,[3] we expect that the millimetre-wave signals rise and decay rapidly. In fact, if an optical pulse train were used to illuminate the waveguide, a millimetre-wave pulse train mimicking the optical pulse train should result. This indeed was the case as shown in Fig. 3. The interpulse spacing of 7 ns in the millimetre-wave pulse train is the same as that in the optical pulse train. Fig 3 also shows that a modulation bandwidth approaching 1 GHz is attainable. The pulse width of the individual pulse is not resolvable in this Figure since the combined response time of the detecting and display system is slower than the expected pulse width of about 200 ps estimated on the basis of the carrier lifetime data.[3] We have devised a correlation technique similar to that used before[3] to measure the pulse width of the coherent millimetre-wave pulse. The measured pulse width is 600 ps, wider than the predicted pulse width by a factor of three. This discrepancy can be resolved by realising that the millimetre-wave pulse is generated by rapid phase modulation of the signal. As a result the pulse is actually 'chirped', i.e. there is a large frequency sweep within the pulse. Group velocity dispersion will broaden the 'chirped' millimetre-wave pulse when it propagates in a positively dispersive guiding structure. Mismatches between the dielectric and metallic waveguides will also contribute to some broadening. Experiments as well as a detailed theoretical calculation are under way to provide more data for a quantitative analysis of the generation and propagation of the 'chirped' millimetre-wave pulse.

In conclusion, we have demonstrated for the first time the generation of a 'chirped' millimetre-wave pulse by an optoelectronic method. Using this technique, the modulation of millimetre-wave signals at 94 GHz with a modulation bandwidth in excess of 1 GHz is readily achievable.

Acknowledgment: This work was supported in part by the Harry Diamonds Laboratory, US Army, and by the Minta Martin Aeronautical Research Fund, College of Engineering, University of Maryland.

MING G. LI
WEI L. CAO
VEERENDRA K. MATHUR
CHI H. LEE

Electrical Engineering Department
University of Maryland
College Park, Maryland 20742, USA

20th April 1982

References

1 LEE, CHI H., MAK, P. S., and DEFONZO, A. P.: 'Optical control of millimetre-wave propagation in dielectric waveguides', *IEEE J. Quantum Electron.*, 1980, QE-16, pp. 277–288
2 LEE, CHI H., MAK, P. S., and DEFONZO, A. P.: 'Millimetre-wave switching by optically generated plasma in silicon', *Electron. Lett.*, 1978, 14, pp 733–734
3 LEE, CHI H., ANTONETTI, A., and MOUROU, G.: 'Measurements of the photoconductive lifetime of carriers in GaAs by optoelectronic gating techniques', *Opt. Commun.*, 1977, 21, pp. 158–161
4 MARCATILI, E. A. J.: 'Dielectric rectangular waveguide and directional coupler for integrated optics', *Bell Syst. Tech. J.*, 1969, 48, pp. 2079–2102
5 JACOBS, H., and CHREPTA, M. M.: 'Electronic phase shift for millimeter-wave semiconductor dielectric integrated circuits', *IEEE Trans.*, 1974, MTT-22, pp. 411–417

0013-5194/82/110454-03$1.50/0

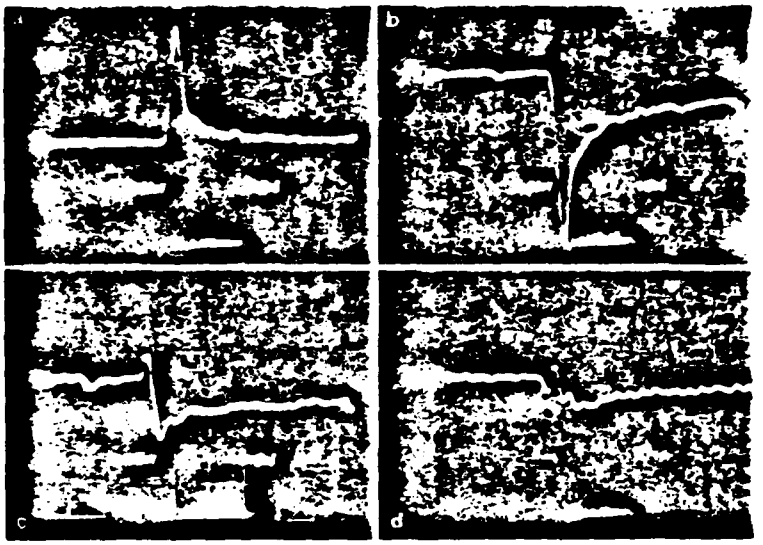

Fig. 3 Experimentally observed millimeter-wave signals corresponding to the theoretical ones depicted in Fig. 2 in the same cyclic order.

wave pulse is actually 'chirped' due to rapid phase modulation. Group velocity dispersion will broaden the 'chirped' millimeter-wave pulse when it propagates through a positively dispersive guiding structure. Mismatches between the dielectric and metallic waveguides will also contribute to some broadening.

Since the millimeter-wave signals are obtained by modulating the dielectric property of the Cr:doped GaAs waveguide, the pulse width of the signals are smaller than the combined response time of the detecting and displaying system. As a result the convenient calibration technique employed in the Si waveguide work [1] to obtain the values of phase shift and attenuation is not directly applicable here. We have, however, developed a dynamic bridge method to determine the values of the laser induced phase shift and attenuation. The output electric field of the bridge (see Fig. 2 of reference 3) is the sum of two phasors, E_A representing the electric field in the arm with dielectric waveguide, and E_B, the RF field in the other arm. E_A and E_B are linearly polarized in the same direction. When the bridge is balanced prior to laser illumination, $E_A = -E_B$ and the output is zero. Under laser illumination E_A is suddenly shifted to a new value and then relaxes back to its initial value as the laser induced carriers decay (represented by the rotation of the E_A phasor in a phasor diagram). The output waveform of the millimeter-wave detector is proportional to $|E_A + E_B|^2$. A positive pulse with a characteristic decay results. The amplitude as well as the detailed temporal profile of the pulse depends upon the initial density of the induced carriers and the material transport parameters. Based on the theoretically calculated curves of phase shift and attenuation as a function of carrier density [4] and assuming a certain decay characteristic of the excess carriers, we have calculated the temporal profile of the signal at the output of the

147

electron-hole plasma resulting in a change of the complex index of refraction of the semiconductor thereby altering the boundary conditions of the waveguide and changing the propagation constant. A millimeter-wave launched into the waveguide experiences amplitude and/or phase modulation while propagating through the illuminated interval. The ratio of amplitude to phase modulation depends on the density and geometry of the plasma. For example, if the density yields a skin depth δ much less than the thickness of the plasma layer, the effect of the plasma is equivalent to an image guide. This yields a nearly pure phase shift, ϕ, given by the relationship

$$\phi = (k_z - k_z')\Delta L. \qquad (1)$$

In general case, the transient response of the millimeter-wave depends upon the transport parameters of the optically induced carriers, such as carrier collision time, mobility, diffusion characteristics, etc. The mechanism for phase shift and attenuation can then be satisfactorily described in terms of a model developed in this work based on Marcatili's approximation [2].

An experiment was performed by using a millimeter-wave bridge similar to that used previously. The GaAs waveguide was inserted in one arm of the bridge. Initially, without laser-pulse illumination of the GaAs, the bridge was balanced by adjusting a mechanical attenuator and phase shifter in the other arm so that there was no signal at the output. When a single picosecond pulse of 0.53 μm extracted from a frequency doubled mode-locked Nd:YAG laser was illuminating the GaAs waveguide, the bridge became unbalanced and coherent signals appeared at the output of the bridge. Because the lifetime of the induced carriers is of the order of 100 picoseconds, the millimeter-wave signals rise and decay rapidly. If an optical pulse train is used to illuminate the waveguide, a millimeter-wave pulse train results mimicking the optical pulse train (see Fig. 3 of reference 3). This feature indicates that a modulation bandwidth approaching 1 GHz is attainable. The pulse width of the individual pulse is not resolvable since the combined response time of the detecting and display system is slower than the expected pulse width of about 200 picoseconds, wider than the predicted pulse width by a factor of three. This discrepancy can be resolved by realizing that the millimeter

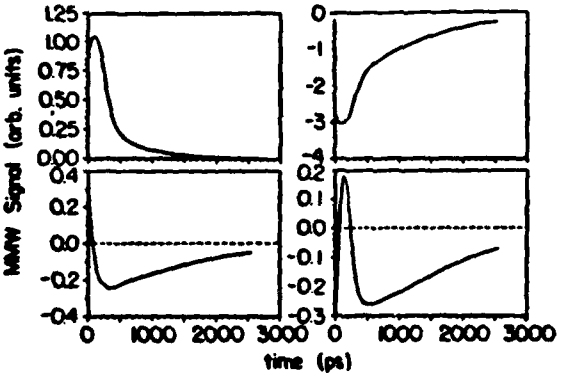

Fig. 2 Theoretical temporal profile of the millimeter-wave signals generated for the unbalanced bridge due to the decay of the optically induced carriers. The curves are plotted for different initial phase angles between the electric fields from two different arms. (a) 180°, the balanced case; (b) 0°; (c) 115°; and (d) 235°.

148

APPENDIX C

Picosecond Optoelectronic Modulation of Millimeter-Waves in GaAs Waveguide

M.G. Li, V.K. Mathur, Wei-Lou Cao and Chi H. Lee

Department of Electrical Engineering, University of Maryland
College Park, MD 20742, USA

Optically controlled microwave or millimeter-wave devices have been a topic of great interest recently. Utilizing a laser induced electron-hole plasma in semiconductor waveguide to control the propagation of an RF signal, we have previously demonstrated the switching, gating and phase shifting of millimeter-wave signal in Si-waveguide with picosecond precision [1]. Phase shifts as large as 300°/cm at 94 GHz were observed. In the experiment involving switching and gating of RF waves, millimeter-wave pulses with pulsewidth as short as 1 ns and variable to tens of nanoseconds have also been generated. In these earlier experiments, high resistivity Si was used as the waveguide material. Since the carrier lifetime in pure silicon is in the millisecond range, to generate a short RF pulse, one generally requires two separate laser pulses, one to "turn on" and the other to "turn off" the millimeter-wave signal. Furthermore, the repetition rate of the device is limited by the carrier recombination rate to less than 10 KHz. In this work, we will report on our most recent study of this type of device by using Cr:doped GaAs as the waveguiding medium. Due to rapid carrier recombination, only a single picosecond optical pulse is needed to produce an ultrashort millimeter-wave pulse. This feature has been utilized to construct a high speed millimeter-wave modulator with a repetition rate well in excess of 1 GHz.

Optical control of RF-waves offers the following advantages: (a) near perfect isolation between the controlling and the controlled devices, (b) low static and dynamic insertion loss, (c) possibility of fast response with picosecond precision, and (d) high power handling capability.

The basic principle of opical control of millimeter waves is illustrated schematically in Fig. 1. The propagation constant, K_z, in an interval ΔL of a rectangular GaAs waveguide (2.4 x 1.0 mm) is changed to K_z' by illuminating the broadwall with optical radiation. The absorbed light generates an

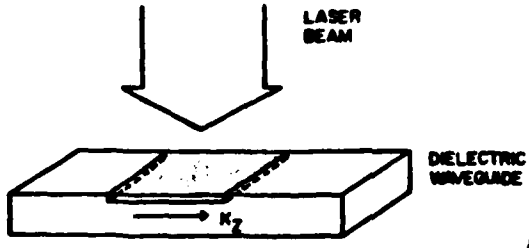

Fig. 1 Schematic diagram of an optically controlled phase shifter, k_z is the propagation vector in the waveguide.

detector. Figure 2 represents the results of these calculations with different initial phase angles between E_A and E_B. Here we have assumed a two component decay mechanism for the carriers with decay constants τ_1=100 ps and τ_2=1000 ps respectively. The mechanism for τ_1 may be due to efficient recombination at chromium impurities; while for τ_2, it may be due to ambipolar diffusion. The laser induced carrier density is estimated to be $2 \times 10^{16}/cm^3$, corresponding to the laser energy of 10μJ. The temporal profile is very sensitive to the initial carrier density from optical injection. Fig. 3 shows the observed millimeter-wave signals corresponding to the theoretical situations depicted in Fig. 2. It is apparent that there is a good qualitative agreement. By comparing the data with the theoretically calculated curve, one can conclude that a phase shift of 270° has been observed. This value compares very favorably with the theoretically expected value of 280° for a plasma column of 2 millimeters in length, or 1400°/cm [4].

In conclusion, we have demonstrated for the first time the generation of 'chirped' millimeter-wave pulses. Using this technique, the modulation of millimeter-wave signals at 94 GHz with modulation bandwidth in excess of 1 GHz is readily achievable. A dynamic bridge method has been developed to measure the phase shift and to monitor the carrier decay kinetics. A two component decay has been observed in a Cr:doped GaAs waveguide.

Acknowledgements are due to Professor C.D. Striffler and A.M. Vaucher for their contributions to these studies.

Work supported in part by the Harry Diamond Laboratory and by the Minta Martin Aeronautical Research Fund, College of Engineering, University of Maryland.

References

1. Chi H. Lee, P.S. Mak and A.P. DeFonzo, IEEE J. Quantum Electron. QE-16, 277 (1980).

2. E.A.J. Marcatili, Bell Syst. Tech. J. 48 2079 (1969).

3. M.G. Li, W.L. Cao, V.K. Mathur and Chi H. Lee, Electron. Lett. to be published.

4. A.M. Vaucher, C.D. Striffler and Chi H. Lee, unpublished.